For Reference

NOT TO BE TAKEN FROM THIS ROOM

For Reference

NOT TO BE TAKEN FROM THIS ROOM

Ex libris
universitatis
albertaensis

UNIVERSITY OF ALBERTA
QUAECUMQUE VERA

University of Alberta
Printing Department

Digitized by the Internet Archive
in 2018 with funding from
University of Alberta Libraries

https://archive.org/details/flowofgassolidsm00sand

Thesis
1963
#61

THE UNIVERSITY OF ALBERTA

FLOW OF GAS-SOLIDS MIXTURES IN A VERTICAL CIRCULAR DUCT:
II THE AERODYNAMIC CHARACTERISTICS OF THE TEST UNIT

A THESIS
SUBMITTED TO THE FACULTY OF GRADUATE STUDIES
IN PARTIAL FULFILMENT OF THE REQUIREMENTS FOR THE DEGREE
OF MASTER OF SCIENCE IN CHEMICAL ENGINEERING

DEPARTMENT OF CHEMICAL AND PETROLEUM ENGINEERING

by

O. SANDALL

EDMONTON, ALBERTA

JANUARY 14, 1963

ABSTRACT

Preliminary to the study of the flow of gas-solids mixtures in a vertical circular duct, its aerodynamic characteristics were investigated. The duct was a 6-inch diameter aluminum pipe, 31.5 feet in length. The entrance to the duct was conical in shape to reduce down to a one inch entry throat.

Velocity profiles were established at a position 50.8 diameters downstream from the entrance to the duct for air flow rates corresponding to Reynolds numbers in the range 900 to 31,000. The measured velocity profiles in the form of a Prandtl universal velocity distribution are compared to profiles measured by other investigators. The ratios of maximum velocities to bulk velocities are also compared to values reported in the literature.

Velocity profiles and point velocities were measured at various distances downstream from the entrance to establish at what flow rates fully developed velocity distributions occurred in test section length from 24.0 diameters to 50.8 diameters. It was found that the flow was fully developed in this section at Reynolds numbers exceeding 11,000.

Pressure drop data were taken to classify the wall roughness of the circular duct. The friction factors calculated from this data and compared to literature values of friction factors indicate that the duct can be classified as a smooth tube.

ACKNOWLEDGEMENTS

The author wishes to express his gratitude to Dr. I.G. Dalla Lana for his guidance and assistance in supervising this investigation.

The author is indebted to the Shell Oil Company of Canada, Limited for the graduate fellowship and to the National Research Council of Canada for financial support.

Acknowledgement is also made to the Aluminum Company of Canada, Limited for donation of the 6-inch aluminum pipe used for this investigation.

TABLE OF CONTENTS

		Page No.
List of Tables		i
List of Figures		ii
List of Plates		iv
I	Introduction	1
II	Literature Review	2
III	Experimental Equipment	6
IV	Experimental Work	14
V	Experimental Results and Discussion of Results	17
VI	Conclusions and Recommendations	36
	Nomenclature	38
	Bibliography	40

Appendices

A	Calibration of the Equipment	43
B	Experimental and Calculated Data	49
C	Conversion of Equipment for Gas-Solids Flow Measurement	84
D	The Problem of Sampling an Air-Solids Stream	89

LIST OF TABLES

Table		Page No.
1-7	Pitot Tube Traverses	51-57
8-15	Hot Wire Traverses	61-68
16-22	Plotting Data for Universal Velocity Distribution	69-75
23	Ratio of Bulk Velocity to Maximum Velocity for Fully Developed Profiles	76
24	Results of Graphical Integrations	76
25	Point Velocity Measurements at 24.0, 41.2 and 50.8 Pipe Diameters Downstream from Entrance	77
26	Friction Factor Data	78
27-28	Hot Wire Calibration	79-80
29	Calibration of 0.375" Orifice	81
30	Effect of Vanes at $Re \cong 1320$	82
31	Effect of Vanes at $Re \cong 1690$	83
32	Effect of Blower Speed on Flow Rate	45
33	Pressure-Recorder Controller Calibration	45
34	Check on Temperature Recorder	46
35	Flow Rates as Calculated by Orifice Plate and From Hot Wire Traverses	47

LIST OF FIGURES

Figure		Page No.
1	Schematic Equipment Diagram	10
2	Pitot Tube	11
3	Hot Wire Probe	11
4	Fully Developed Velocity Profiles	25
5	Velocity Profiles at Low Flow Rates	26
6	Comparison of Velocity Profiles with Universal Velocity Distribution for Smooth Tubes	27
7	Ratio of Average to Maximum Velocity versus Reynolds No.	28
8	Velocity Profile for Re = 11,430 Measured at Distances of 50.8 and 24.0 Pipe Diameters Downstream From the Entrance	29
9	Development of Velocity Profile at Re = 9660	30
10	Axis Velocity Measurements at 24.0, 41.2 and 50.8 Pipe Diameters Downstream from the Entrance	31
11	Experimental Profile Compared to Theoretical Fully Developed Profile for Re = 925	32
12	Effect of Corner Vanes at Re = 1320	33
13	Effect of Corner Vanes at Re = 1690	34
14	Friction Factor versus Reynolds Number	35
15	Calibration of Hot Wire Probe	60

16 Solids Sampling Arrangement 90

17 Errors Due to Non-Isokinetic Sampling 91

18 Effect of Probe Diameter on Solids Concentration Under Isokinetic Conditions 92

LIST OF PLATES

Plate		Page No.
1	Entrance Section	12
2	Probe Mount Arrangement on 6-inch Aluminum Pipe	13
3	Solids Separation Section	88

I INTRODUCTION

A long-term project to study the flow characteristics of an air-solids mixture in a vertical circular duct has been initiated at the University of Alberta. The project is sponsored by the National Research Council of Canada.

Equipment has been designed and constructed to investigate flow rates corresponding to air Reynolds numbers of up to 35,000 and various solids to air mass loading ratios. The test duct consisted of a 6-inch aluminum pipe, 31.5 feet long, with a diverging conical entrance and a converging conical exit section. The major design of this equipment was carried out by B. Bowers (1).

The purpose of the author's investigation was to determine the aerodynamic characteristics of the test unit preliminary to the study of air-solids flow. It was desired to establish velocity profiles for air alone for future comparison with air velocity profiles measured in the presence of solid particles. This work is also concerned with the hydrodynamic starting length and the entrance effects as other important characteristics of the test unit to be determined before studying the flow of air-solids mixtures.

II LITERATURE REVIEW

Various correlations for fully developed turbulent velocity profiles in smooth tubes can be found in the literature. Probably the most well known and widely employed of these correlations is the universal velocity distribution for smooth tubes which is based on either Prandtl's (2) or von Karman's (3) logarithmic velocity distribution equation.

Prandtl, using his mixing length theory as a basis and assuming that the mixing length is proportional to the distance from the wall derived the expression:

$$u = u_m + 2.5\, u^* \ln y/h \tag{1}$$

The derivation is for the case of flow along a smooth flat wall. However, the equation is used to correlate experimental velocity profiles obtained in smooth pipes by substituting the pipe radius, r_w, for the distance, h.

Prandtl's logarithmic velocity distribution equation can be further extended to yield the universal velocity distribution for smooth tubes by assuming that the velocity gradient within the laminar film is constant and that the transition to fully developed turbulence occurs abruptly at some point a distance from the wall, i.e. there is no gradual transition from laminar to turbulent flow:

$$u^+ = c + 2.5 \ln y^+ \tag{2}$$

Nikuradse (2) experimentally determined the value for the constant, c, in equation 2 to be 5.5.

Equation 2 represents data in the turbulent core. The turbulent core being arbitrarily defined to occur at values of y^+ greater than 30. The velocity distribution in the laminar film and in the buffer layer is usually represented by two other curves (3):

$$0 < y^+ < 5.5 \text{ (laminar layer)}, \quad u^+ = y^+ \tag{3}$$

$$5.5 < y^+ < 30 \text{ (buffer layer)}, \quad u^+ = -3.05 + 2.4 \ln y^+ \tag{4}$$

Deissler (5) found values for the constants in equation 2 different from those found by Nikuradse. Deissler, studying the adiabatic flow of air in a smooth tube over the Reynolds number range 10,000 to 200,000, obtained for values of y^+ greater than 30 the equation:

$$u^+ = 3.8 + 2.78\ y^+ \tag{5}$$

Rothfus and Monrad (4) noted a systematic deviation from equation 2 of experimental data in the Reynolds number range of 3,000 to 25,000. They empirically modified the conventional coordinates, u^+ and y^+, by multiplying u^+ by U/u_m and y^+ by u_m/U, and obtained a better correlation, particularily in the Reynolds number range 3,000 to 4,000.

In order to use equations 2 or 5 for the correlation of turbulent velocity profiles, it is necessary to have pressure drop data in order to determine the so-called friction velocity, u^*. In this regard, Campbell and Brebner (6) have measured pressure

drops for the flow of water in a 6-inch aluminum pipe. Their results indicate that the friction factor for 6-inch aluminum pipe lies close to the friction factor for smooth pipes as given by Moody (7). Moody's friction factor is defined as:

$$f = \frac{2g_c D}{\rho U^2} \frac{dP_f}{dL} \tag{6}$$

Literature values for the entrance length required for the development of fully developed turbulent velocity profiles are varied. Schiller and Kirsten (2) found that lengths of 50 diameters and greater were necessary for the attainment of fully developed velocity profiles for turbulent flow at Reynolds numbers greater than 10,000. Nikuradse's (8) experiments show that the final velocity distribution is reached in a distance of 25 to 40 diameters. Diessler (9), using a rounded entrance, found that for a Reynolds number of 10,000 an entrance length of 22.9 diameters was required and for a Reynolds number of 30,000 a length of 31.1 diameters was required. A still shorter transition length is given by the theory of Latzko (9) who predicted the relationship:

$$X/D = 0.623\ (Re)^{\frac{1}{4}} \tag{7}$$

According to this relationship the final velocity distribution is reached in a distance of about 6 diameters for a Reynolds number of 10,000.

Thus it seems that there is no reliable relationship available

to predict, for all situations, the distance required for development of a turbulent velocity profile and the distance must be determined by experiment. The distance required appears to be a function of entrance conditions and is less dependent on the Reynolds number than for the case of laminar flow. Usually the starting length required for turbulent flow is considerably shorter than that required for laminar flow (8).

In the case of laminar flow, Langhaar's (10) analysis shows that,

$$X/D \cong 0.0575\ Re \tag{8}$$

Boussinesq's (8) prediction gives a slightly longer hydrodynamic starting length for laminar flow,

$$X/D \cong 0.065\ Re$$

Both of these predictions are for the case of equal point velocities across the inlet cross section.

III EXPERIMENTAL EQUIPMENT

The equipment was designed to study air-solids flow characteristics for air flow rates corresponding to comparatively low Reynolds numbers up to approximately 35,000. The equipment is shown schematically in Figure 1.

Air to the system was supplied by a low pressure 0-1750 rpm Roots-Connersville rotary positive blower. The air flow rates were controlled by a Foxboro Model M40 pneumatic controller. The pressure in the test section could also be controlled from 0 to 3 psig by a Foxboro Model M40 pneumatic controller, however, all tests were made with pressures in the test section close to atmospheric pressure. Air temperatures were measured downstream from the orifice flange with an iron-constantan thermocouple and a Brown electronic temperature recorder.

All flow rates could be reproduced by the air weight-rate recorder-controller in the Reynolds number range of about 9000 and higher by setting the blower speed. The orifice plate of 1.544 inches was too large for good control in the lower range because of the small pressure drops across the orifice. It was necessary to use a smaller orifice of 0.375 inches diameter. This smaller orifice was calibrated in place with a displacement meter. Flow rates in the range of Reynolds numbers from 925 to

2840 were set by direct measurement of the pressure drop across this 0.375 inch orifice.

The test duct consisted of a circular aluminum tube 31.5 feet long having an internal diameter of 6.255 inches and a wall thickness of 0.203 inches. Entrance and exit cones were machined from a mild steel to reduce down from the test section to a one inch throat entrance and a 2-inch diameter exit section. The enclosed angle of the entrance cone was 6 degrees and the enclosed angle for the exit cone was 10 degrees. The 2½-inch entrance section contained the orifice meter with an upstream run of 30 diameters which conformed to American Gas Association standards. The equipment after the exit section included the solids separation apparatus (as outlined in Appendix C). The test section was tapped at five positions for air velocity measurement. These taps were located 12.5, 17.5, 21.5 and 26.5 feet downstream from the entrance.

The entrance to the test section consisted of a 2½-inch tee, a venturi nozzle for introducing solids, and a 2½ - to 6-inch entrance cone. It was found that velocity profiles measured at low flow rates were unsymmetrical and for this reason corner vanes were constructed to fit inside the 2½-inch tee. The vanes were simply constructed from a length of 2-inch pipe cut at 45 degrees and notched on the 45 degree cut to wedge the 12 guage galvanized sheet iron vanes.

The venturi nozzle and entrance cone were machined in sections from mild steel. A problem was encountered in the construction of the entrance cone in that the silver-soldered joints were subject to failures. To overcome this difficulty the joints were subsequently notched and electric-arc welded on the outer surface only as were all joints of the nozzle and exit cones. The nozzle and cones were painted with an aluminum paint on the outside and with an urethane base paint on the inside for protection against corrosion. The entrance section is shown in Plate 1.

A more detailed description, including machine drawings, of the major equipment is given by Bowers (1).

Velocity measurements were made with a pitot tube and micromanometer and also with a hot wire anemometer. The pitot tube design was taken from a small-scale copy (0.535 to 1) of the National Physical Laboratory standard pitot tube. An absolute calibration of this small-scale copy pitot tube has been carried out by Ower and Johansen (11). Impact pressure differences obtained with the pitot tube were measured with a micromanometer (Model MM3) purchased from Flow Corporation. The micromanometer allowed pressure differences to be measured to ± 0.0002 inches of n-butyl alcohol (density = 0.8176 gm./cc at 50 F.). The hot wire anemometer (model HWB2) and the hot wire probe (HWP-A) were also purchased from Flow Corporation. The dimensions of the pitot tube and the

hot wire probe are given in Figures 2 and 3.

The pitot tube was preferable to the hot wire anemometer for air velocity measurements higher than about 3.0 ft./sec. since the pitot tube was considered to be the standard and was used to calibrate the hot wire anemometer. The hot wire anemometer was used at lower velocities because of the limitations in measuring pressure differences with the micromanometer.

Either velocity measuring probe could be positioned in the main flow stream with the probe mount arrangement shown in Plate 2. The use of this probe mount allowed the position of the probes within the flow stream to be set to an accuracy of one - one hundredth of an inch.

FIGURE 1

SCHEMATIC EQUIPMENT DIAGRAM

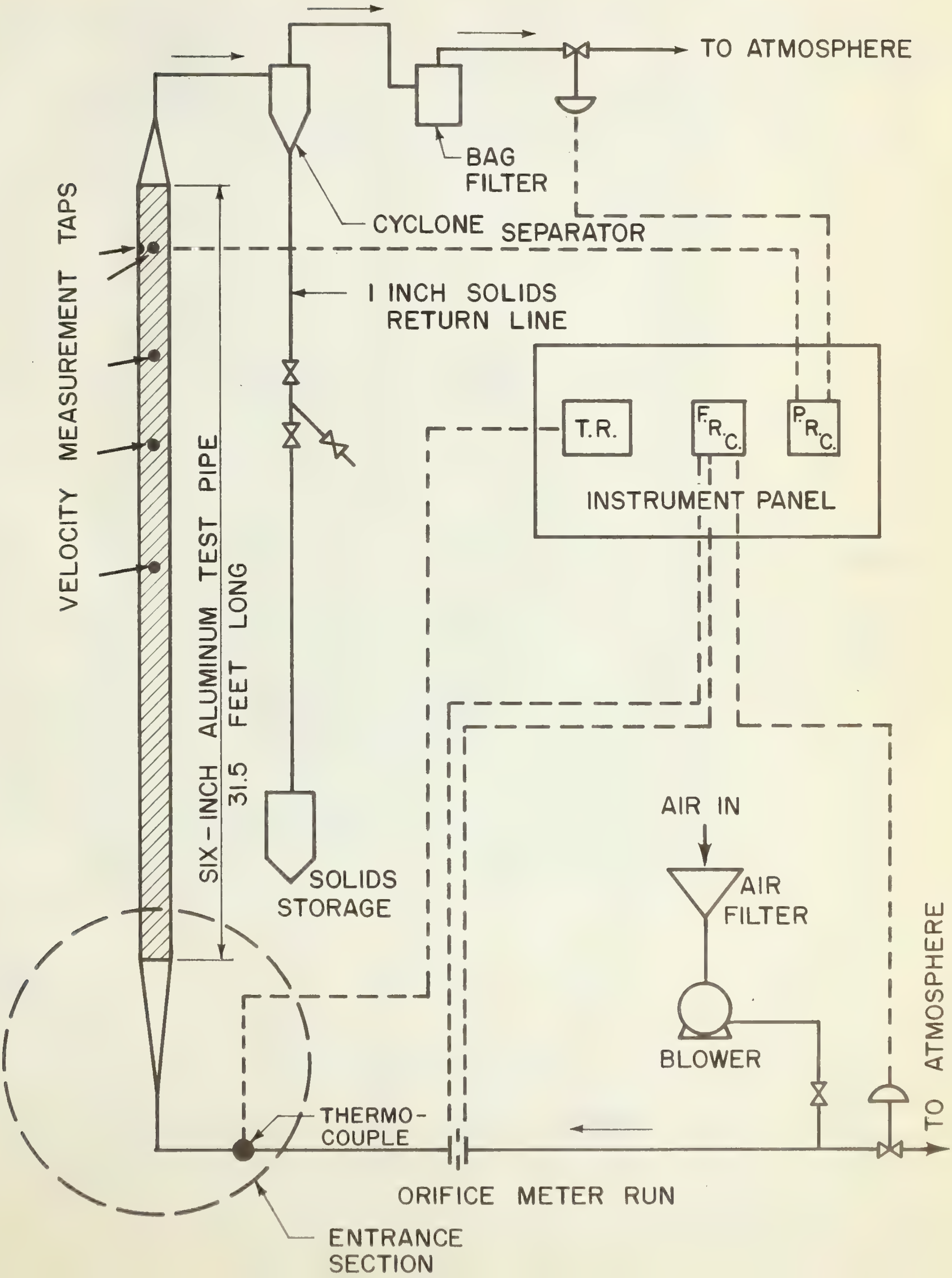

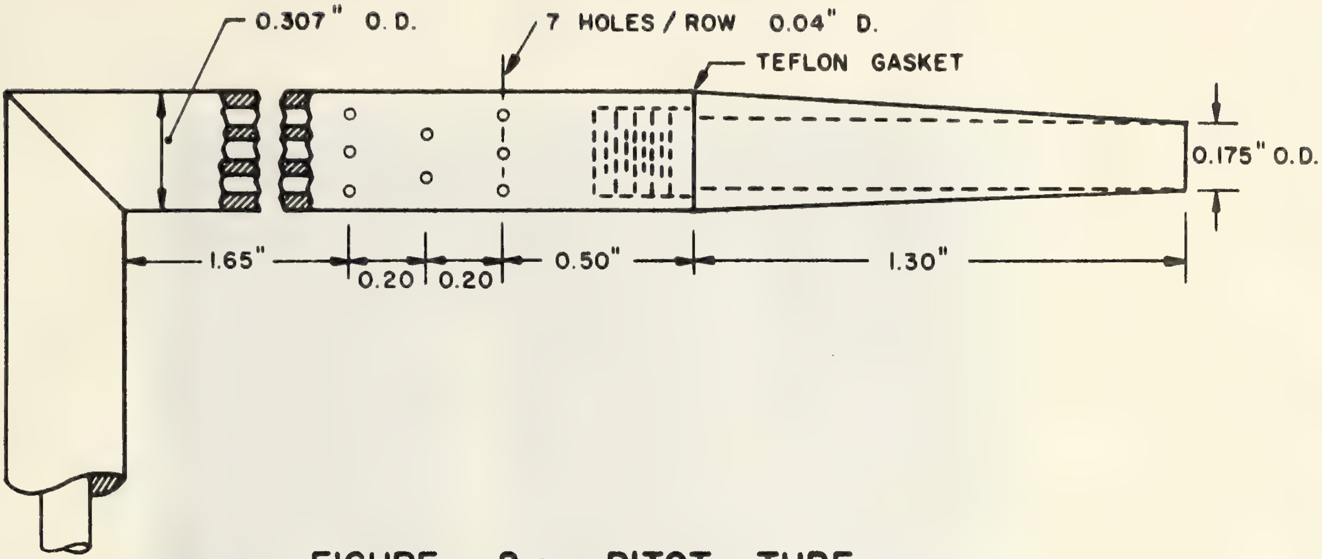

FIGURE 2: PITOT TUBE

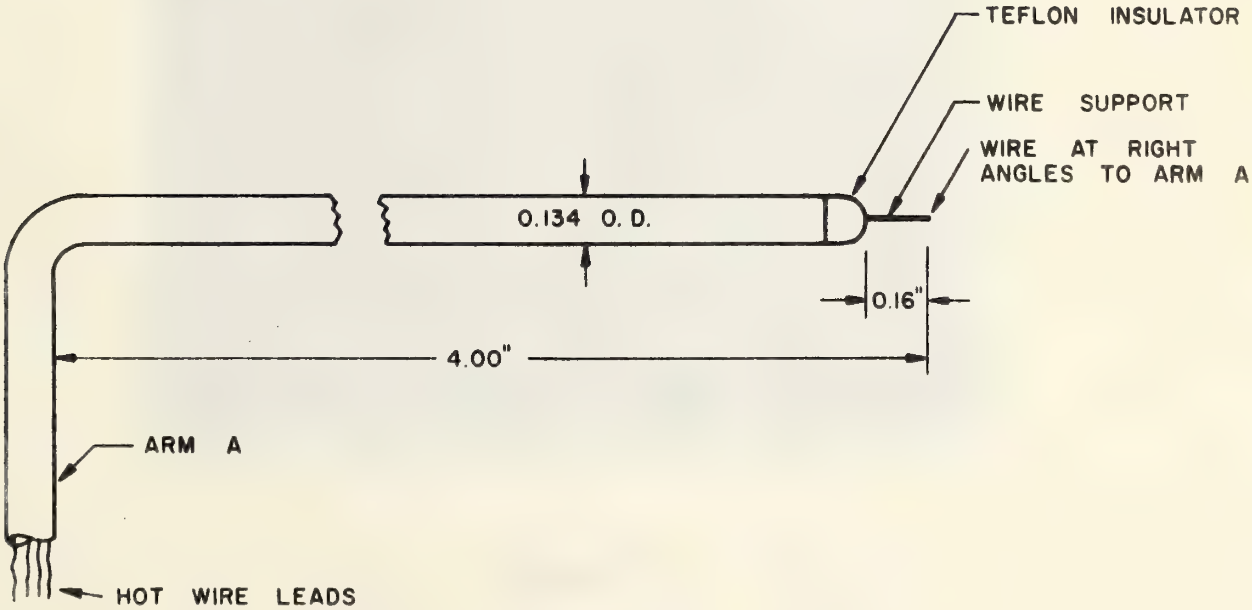

FIGURE 3: HOT WIRE PROBE

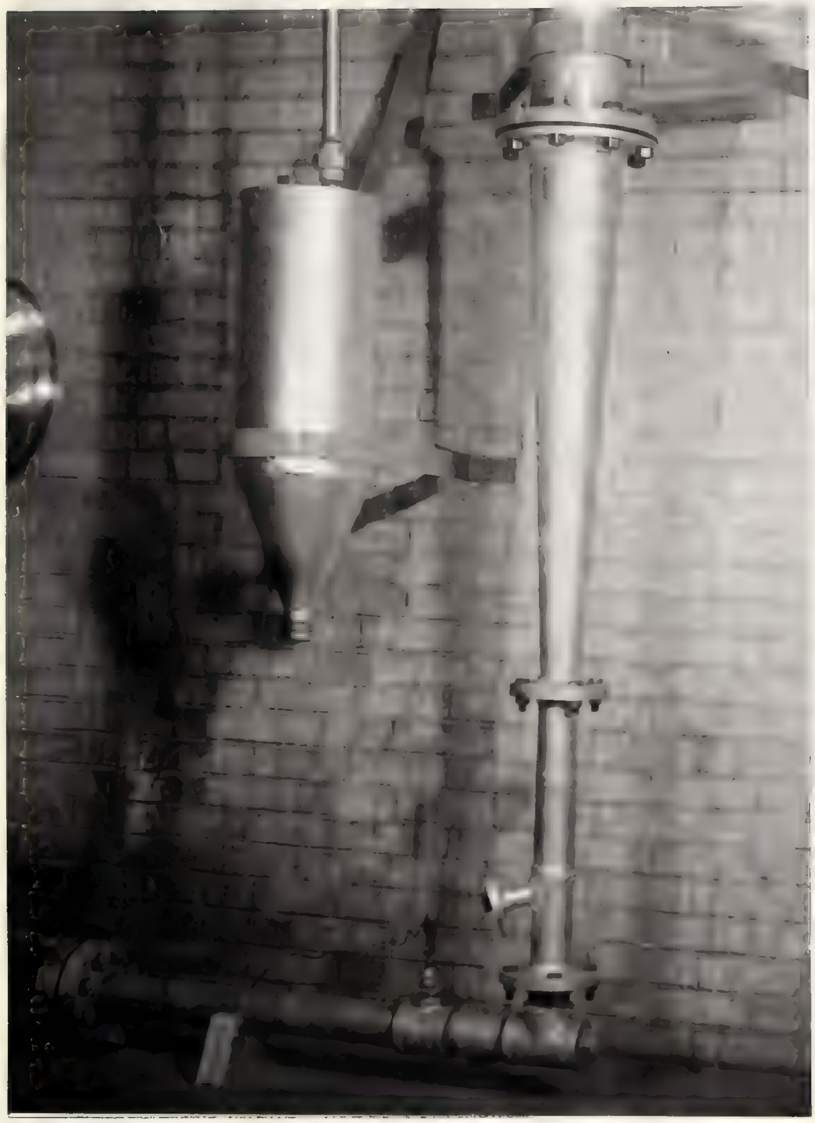

PLATE 1

ENTRANCE SECTION

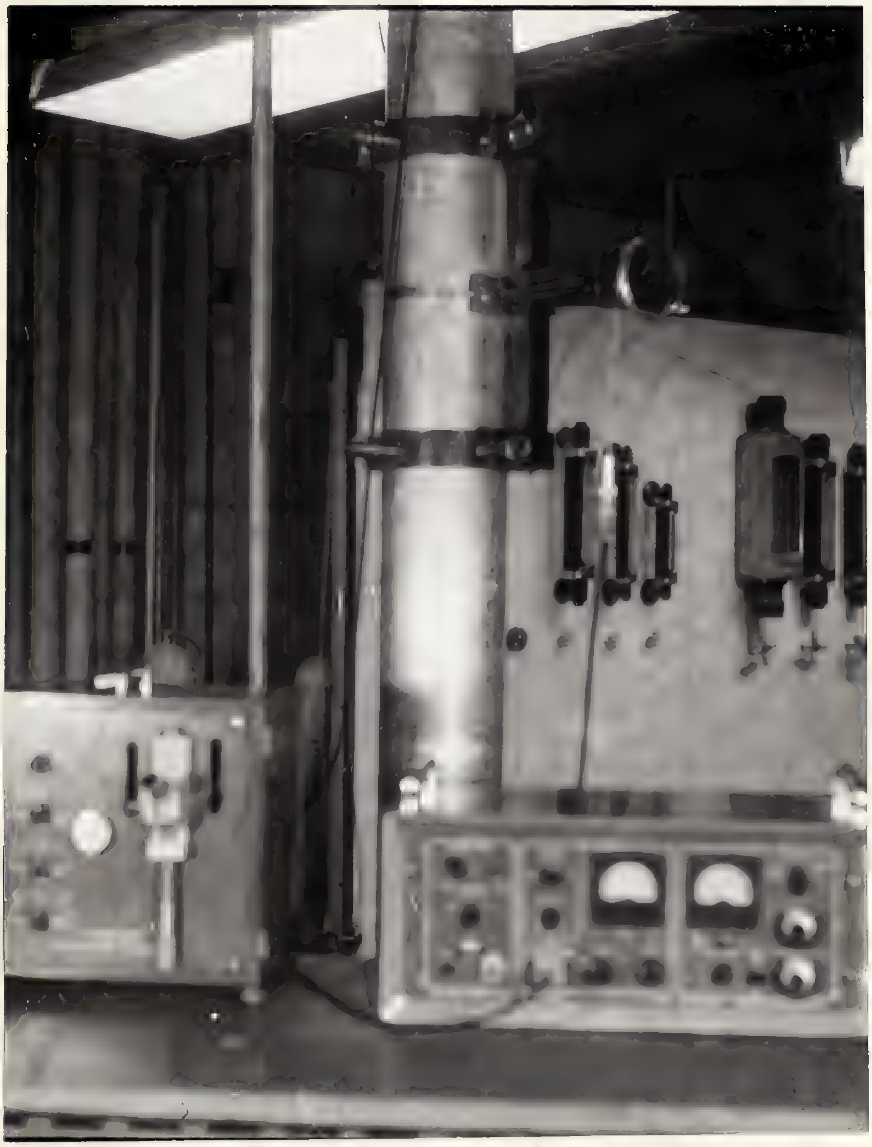

PLATE 2

PROBE MOUNT ARRANGEMENT ON 6-INCH ALUMINUM PIPE

IV EXPERIMENTAL WORK

The following list of equipment was first calibrated as outlined in Appendix A:

1. Air Weight-Rate Recorder-Controller
2. Pressure Recorder-Controller
3. Temperature-Recorder
4. Hot-Wire Anemometer

The calibration curve for the hot wire anemometer probe is presented in Figure 15 of Appendix B. The micromanometer used in this work was not calibrated since it was considered to be the standard for the air velocity measurements.

Velocity profiles were measured at a distance of 50.8 diameters downstream from the entrance of the aluminum tube over the Reynolds number range of about 11,000 to 31,000 using the pitot tube and micromanometer. The use of the pitot tube allowed point velocity measurements to be made at distances of 0.153 inches and further from the wall. The Reynolds number range of velocity profile measurement was extended to a Reynolds number of 925 with the use of the hot wire anemometer. Velocity measurements could be taken as close to the wall as 0.067 inches with the hot wire probe.

The upper flow rate range was limited by the capacity of

the blower. Flow rates below a Reynolds number of 925 were not considered since the error in velocities measured with the hot wire anemometer increases as the velocity decreases. The percentage error is about ± 20 per cent in a measured velocity equal to the average velocity for a Reynolds number of 925. All profiles were measured under the conditions of atmospheric pressure and temperatures close to room temperature. During the tests, atmospheric pressure varied between 69.35 and 71.48 centimeters of mercury and the flowing air temperatures ranged from 18.5 to 27.5 degrees Centigrade.

At the flow rate corresponding to a Reynolds number of 30,800 and at a distance of 50.8 pipe diameters downstream from the entrance, pitot tube traverses were taken at right angles to each other. This was done to assure that the velocity profiles obtained were symmetrical in all directions about the tube axis.

Velocity profiles measured at flow rates corresponding to Reynolds numbers of 1300 and lower were found to be unsymmetrical. The distorted velocity distributions were due to the 90 degree change in direction of flow through the entrance tee. Corner vanes were designed and built to fit into the entrance tee. The use of these corner vanes resulted in symmetrical profiles at the lower flow rates and did not affect the shape of the velocity profiles at higher flow rates.

Velocity profiles and point velocities were measured with the hot wire anemometer and with the pitot tube at distances of 24.0, 41.2, and 50.8 pipe diameters downstream from the entrance to establish at what flow rates fully developed flow existed in the test section between these lengths.

Pressure drop data were obtained for seven flow rates that were considered to be fully developed. The pressure drop was measured with the micromanometer between two points a distance of 18.416 feet apart. The points were located 24.0 and 59.3 pipe diameters downstream from the entrance. The purpose of the pressure drop tests was to verify that the pipe could be classified as a smooth tube.

V EXPERIMENTAL RESULTS AND DISCUSSION OF RESULTS

A. Velocity Profiles:

The velocity profiles obtained at a distance of 50.8 diameters downstream from the entrance of the 6-inch aluminum pipe are shown in Figures 4 and 5. The profiles were measured over the Reynolds number range of 925 to 30,800. The velocity profile determined at a Reynolds number of 11,430 was measured at distances of 24.0 and 50.8 diameters downstream from the entrance and the profiles obtained were found to be the same at both sections. It was thus concluded that the velocity profiles for higher Reynolds numbers measured at the section 50.8 diameters downstream were fully developed. Experimental and calculated data for the velocity profiles are found in Tables 1 to 15 of Appendix B. The method of calculating the air velocity from pitot tube measurements is outlined on page 50 of Appendix B and the method used for hot wire anemometer calculations is outlined on page 58 of Appendix B.

The velocity profiles that were considered to be fully developed were plotted using dimensionless coordinates, u^+ versus y^+, and are compared in Figure 6 to the universal velocity distribution for smooth tubes as found by Nikuradse (2) and by Deissler (5). The definitions of the dimensionless

velocity, u^+, and the dimensionless distance, y^+, are as follows:

$$u^+ = u/u^*$$

$$\text{where,}\quad u^* = \sqrt{\frac{\tau_w g_c}{\rho}} = \sqrt{f/8}\;U$$

$$\text{and}\quad y^+ = yu^*/\nu$$

The friction factors used for these calculations were obtained from the Blasius (2) friction factor curve for smooth pipes. The calculated dimensionless coordinates may be found in Tables 16 to 22 of Appendix B.

The experimental data plotted in this dimensionless form appear to be scattered about Nikuradse's and Deissler's lines. Deissler's line was determined for the adiabatic flow of air in a smooth tube over the Reynolds number range of 10,000 to 200,000. His data at values of y^+ greater than 30 (velocities measured in the turbulent layer) fit the equation,

$$u^+ = 3.8 + 2.78 \ln y^+$$

Deissler's points had a maximum deviation of 5 per cent from this curve. The data obtained in this work and plotted on the same graph are never more than 5 per cent off Deissler's line except for points evaluated next to the wall.

It has been found (2), however, that velocities measured near the wall with pitot tubes give velocity values that are too high. This error occurs near the wall because the velocity

gradient is quite steep and therefore, the impact pressure will also have a high gradient near the wall. The impact pressure measured with a pitot tube should be the average value over the pitot tube opening but this average does not correspond to the point velocity at the center of the pitot tube opening but corresponds to a velocity that is higher. The pressure gradient across the pitot tube opening may also cause circulation within the pitot tube tip and this circulation would result in an even higher measured impact pressure. This would account for the deviation of points evaluated nearest the wall.

The ratio of bulk velocity to maximum velocity was calculated for each of the velocity profiles that were considered to be fully developed. These values are tabulated in Table 23 of Appendix B and are compared with published values in Figure 7. The measured ratios are slightly higher than those found by Stanton and Pannell (2) for air flow and are slightly lower than the values found by Nikurandse (4) for water flow.

The bulk velocities and thus the Reynolds numbers were determined by plotting the product of the point velocity times the radius versus the radius and graphically integrating to determine the value of the integral:

$$\int_0^{r_w} urdr$$

A planimeter was used for the graphical integrations. The bulk velocity is found from:

$$U = \frac{2\pi}{A} \int_0^{r_w} urdr$$

Tabulated values of the results of the graphical integrations are found in Table 24 of Appendix B.

B. Hydrodynamic Starting Length and Entrance Effects:

The velocity profile obtained at a Reynolds number of 11,430 was reproduced at distances of 24.0 and 50.8 pipe diameters downstream from the entrance. These profiles were found to agree within the experimental error of the micromanometer and are shown in Figure 8. This indicates that the hydrodynamic starting length for this system is 24.0 pipe diameters or less, for a Reynolds number of 11,430. This compares to the findings of Deissler (9) who found, for a rounded entrance, that a starting length of 22.9 diameters was required for a Reynolds number of 10,000.

The flatness of the velocity profiles measured at the 50.8 diameter section at Reynolds numbers lower than 11,430 indicated that these profiles were not fully developed. The velocity profile obtained at a Reynolds number of 9,660 was repeated at a distance of 24.0 pipe diameters downstream from the entrance and the profile at this section was found to be significantly flatter than the profile obtained 50.8 diameters

downstream. Therefore, the starting length for flow at a Reynolds number of 9,660 exceeds 24.0 pipe diameters.

For laminar flow, the starting length is expected to be proportional to Reynolds number and to be longer than for turbulent flow (8). For turbulent flow, the starting length is proportional to some fractional power of the Reynolds number as indicated by Latsko (9). Since flow at a Reynolds number of 9,660 has a longer starting length than for flow at a Reynolds number of 11,430, it seems that there is some transition in the starting length function of Reynolds number in this range of flow rates. The effect of the degree of turbulence on the starting length must be significant in this region.

Point velocities were measured at flow rates corresponding to Reynolds numbers above 11,000 with the pitot tube and micromanometer at the axis of the pipe at distances of 24.0 and 41.2 pipe diameters downstream from the entrance and were compared to the point velocities as measured by the hot wire anemometer at a distance of 50.8 diameters downstream from the entrance. The results as shown in Figure 10 show good agreement, indicating that fully developed flow existed in the test section between 24.0 and 50.8 diameters over the range of flow rates investigated. The experimental and calculated data appear in Table 25 of Appendix B.

The velocity profiles measured at Reynolds numbers below 11,430 become flatter as the Reynolds number decreases with the exception of the profile obtained for the lowest Reynolds number of 925. This is to be expected since for laminar flow the hydrodynamic starting length has been found to be proportional to the Reynolds number, i.e. as the Reynolds number decreases the starting length decreases. The predictions of Boussinesq (8) and Langhaar (10) for conditions of equal velocity at all points across the entrance cross-section are:

$X/D = 0.065\ Re$ (Bousinesq)

and, $X/D = 0.0575\ Re$ (Langhaar)

where, X = distance downstream from entrance, ft.

D = diameter of pipe, ft.

According to these predictions, distances of 60.1 and 53.1 pipe diameters would be required for fully developed flow at a Reynolds number of 925 and since this profile was measured at a distance of 50.8 pipe diameters downstream from the entrance, it is not expected to be fully developed. The measured profile is compared in Figure 11 to the theoretical fully developed laminar profile and it can be seen that the profile is not fully developed.

Early in the work, velocity profiles measured at Reynolds numbers of 1,320 and lower were found to be unsymmetrical. The

installation of corner vanes in the entrance tee resulted in symmetrical profiles being obtained. The profiles at a Reynolds number of 1,320 measured with and without the corner vanes are presented in Figure 12. It can be seen from Figure 13 that the corner vanes have no effect on the velocity profiles measured at Reynolds numbers of 1,690 and higher. It is thought that the degree of turbulence in the entrance nozzle throat is sufficiently high at Reynolds numbers of 1,690 and higher to overcome the distorted velocity distribution entering the nozzle. The distorted velocity distribution entering the nozzle is due to the 90 degree change in direction of flow through the entrance tee.

C. Friction Factor Data:

Pressure drop measurements were taken across the pipe length from 24.0 to 59.3 diameters downstream from the entrance, for flow rates that were considered to be in the fully developed range. If the assumption is made that the density of air in the micromanometer lines is equal to the air density in the test section, the pressure drop that is measured by the micromanometer is the pressure drop due to friction. The experimental and calculated data are found in Table 26 of Appendix B.

The friction factor was calculated and the results were compared to values for smooth pipes found in the literature. The data as presented in Figure 14 shows a fair degree of scatter. It was felt, however, that the curve of Blasius (2) for smooth tubes gave the best fit. This compares with the results of Campbell and Brebner (6) who found, using aluminum pipe of 2, 4 and 6-inch diameters, that the friction factor lies on or sensibly close to the smooth pipe curve given by Moody (7). The point obtained for a Reynolds number of 30,800 seems high compared to the other points obtained. This could be explained if the flow at this Reynolds number was not fully developed in the test section between the pressure taps, i.e. part of the pressure drop measured could be due to a change in the kinetic energy of flow between the sections tapped.

The friction factors used for plotting the velocity profiles in dimensionless form were obtained from the curve of Blasius.

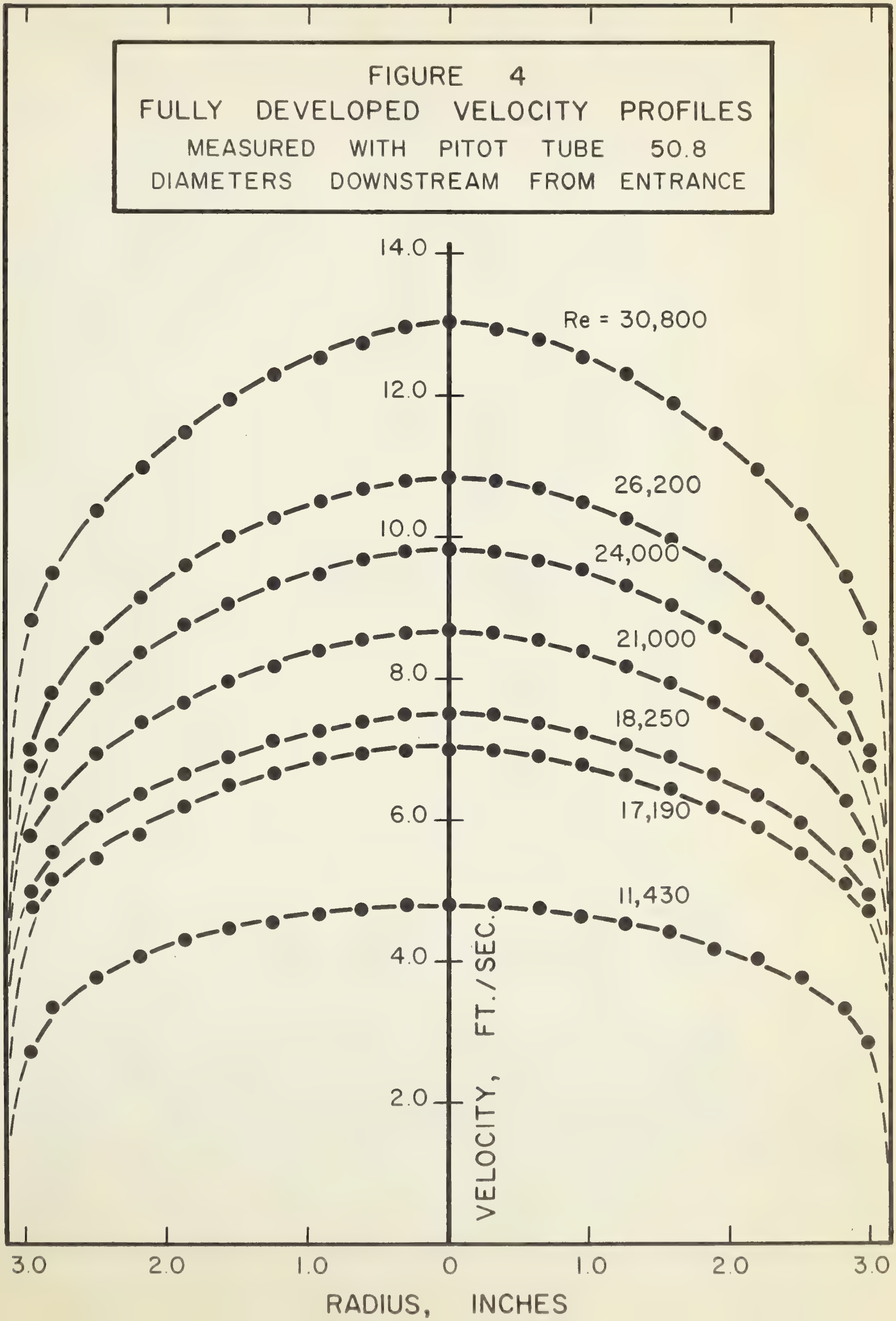

FIGURE 4
FULLY DEVELOPED VELOCITY PROFILES
MEASURED WITH PITOT TUBE 50.8
DIAMETERS DOWNSTREAM FROM ENTRANCE

FIGURE 5
VELOCITY PROFILES AT LOW FLOW RATES
MEASURED WITH HOT WIRE ANEMOMETER
50.8 DIAMETERS DOWNSTREAM FROM ENTRANCE

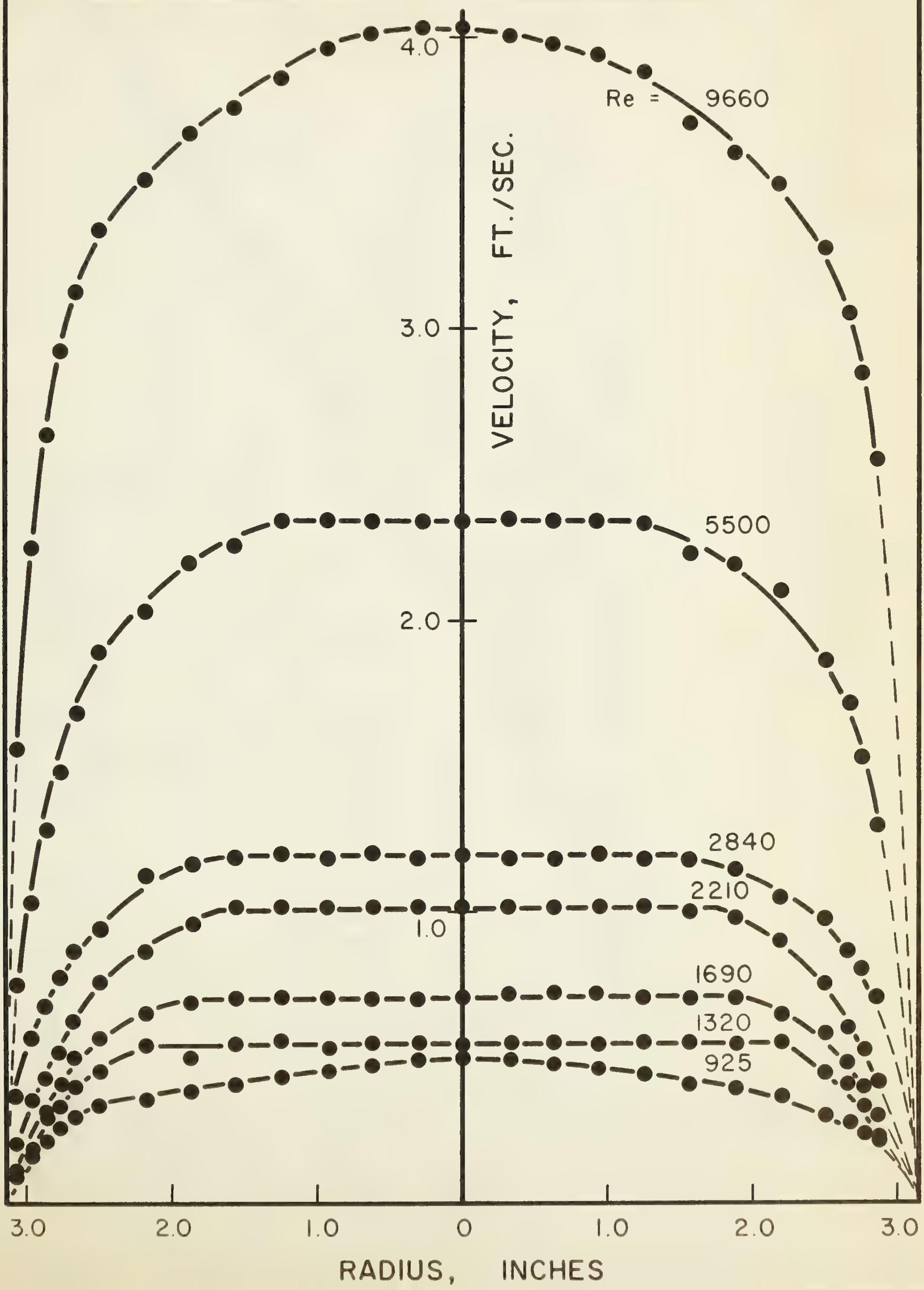

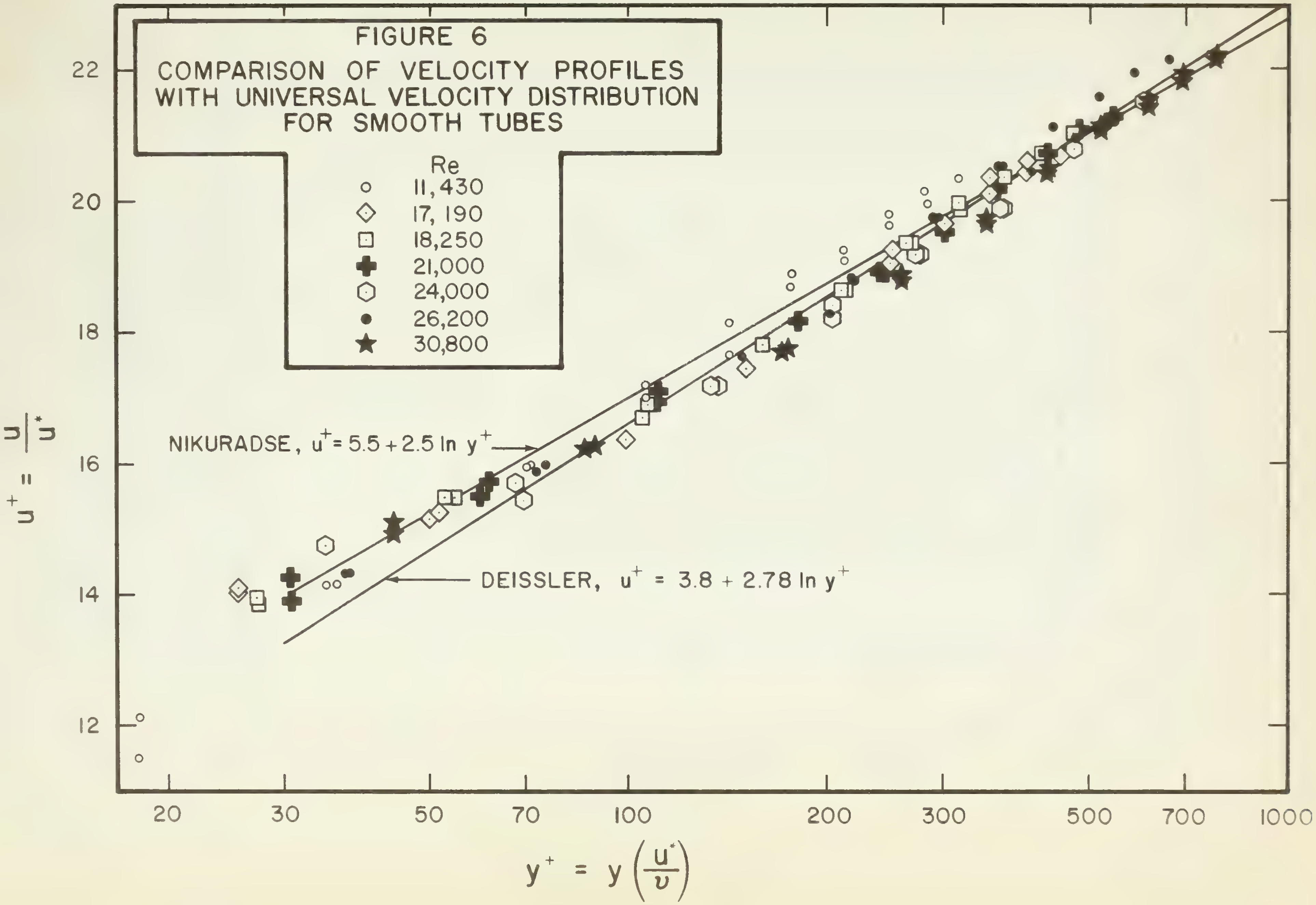

FIGURE 6

COMPARISON OF VELOCITY PROFILES WITH UNIVERSAL VELOCITY DISTRIBUTION FOR SMOOTH TUBES

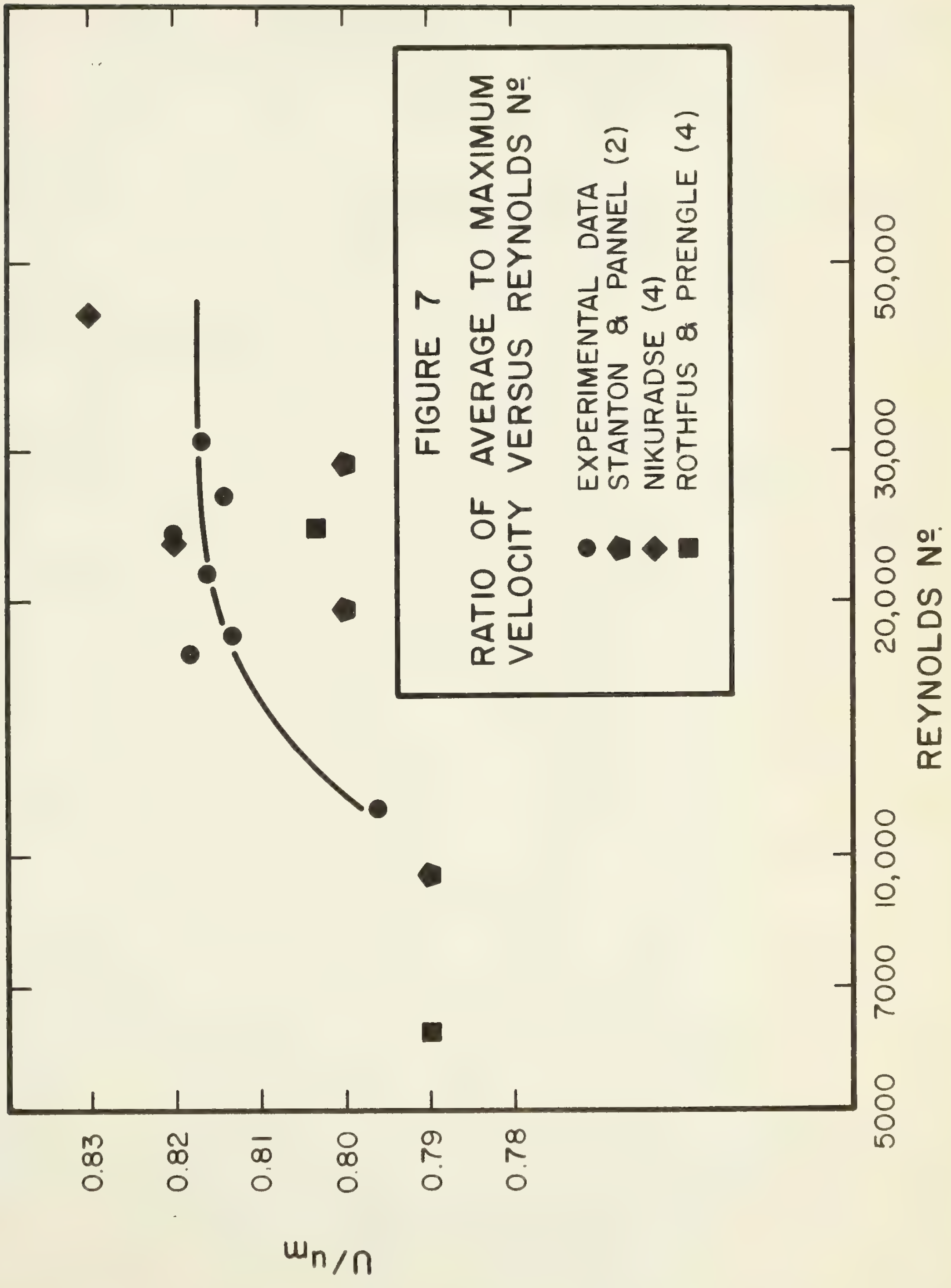

FIGURE 7

RATIO OF AVERAGE TO MAXIMUM VELOCITY VERSUS REYNOLDS No.

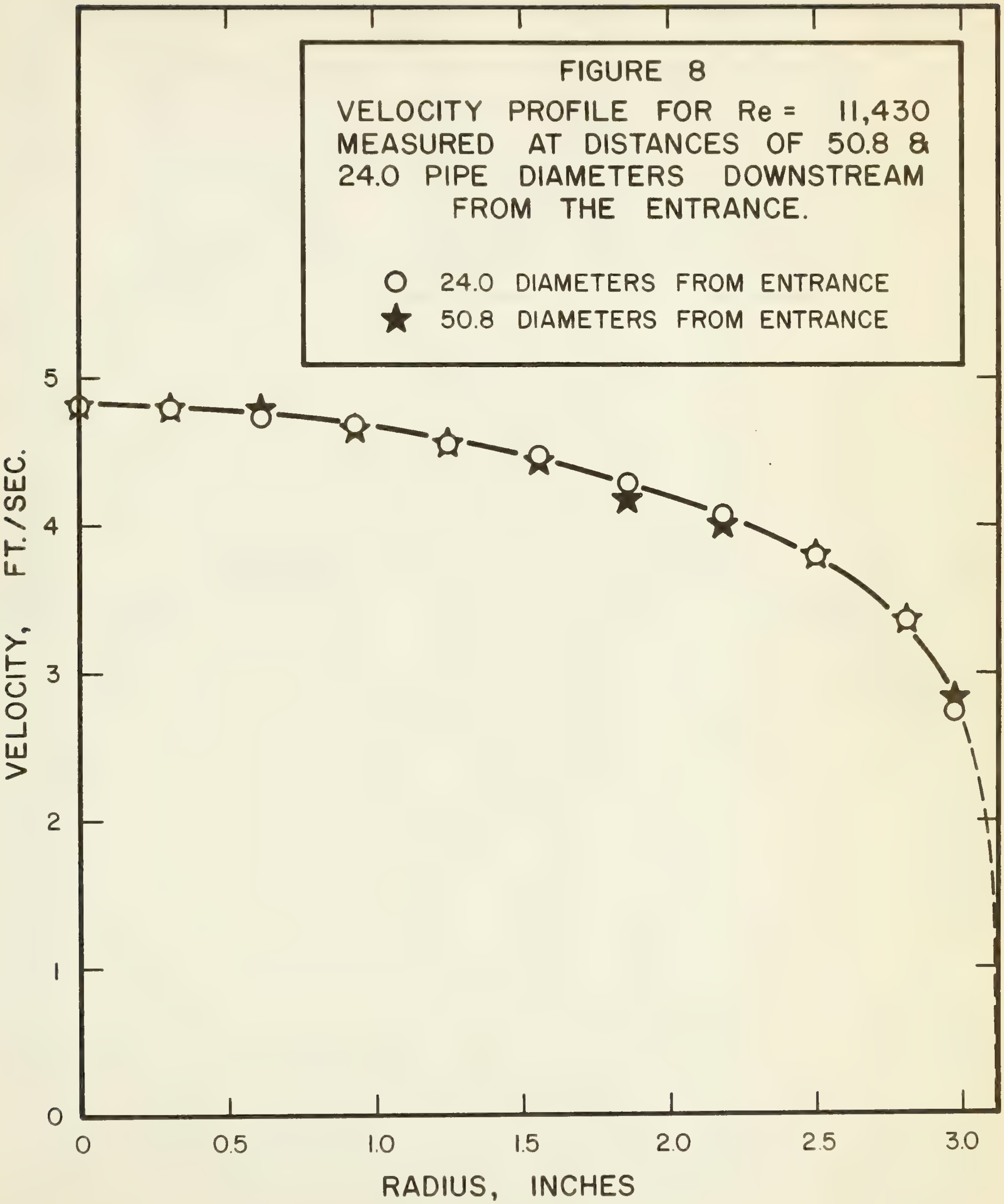

FIGURE 8

VELOCITY PROFILE FOR Re = 11,430 MEASURED AT DISTANCES OF 50.8 & 24.0 PIPE DIAMETERS DOWNSTREAM FROM THE ENTRANCE.

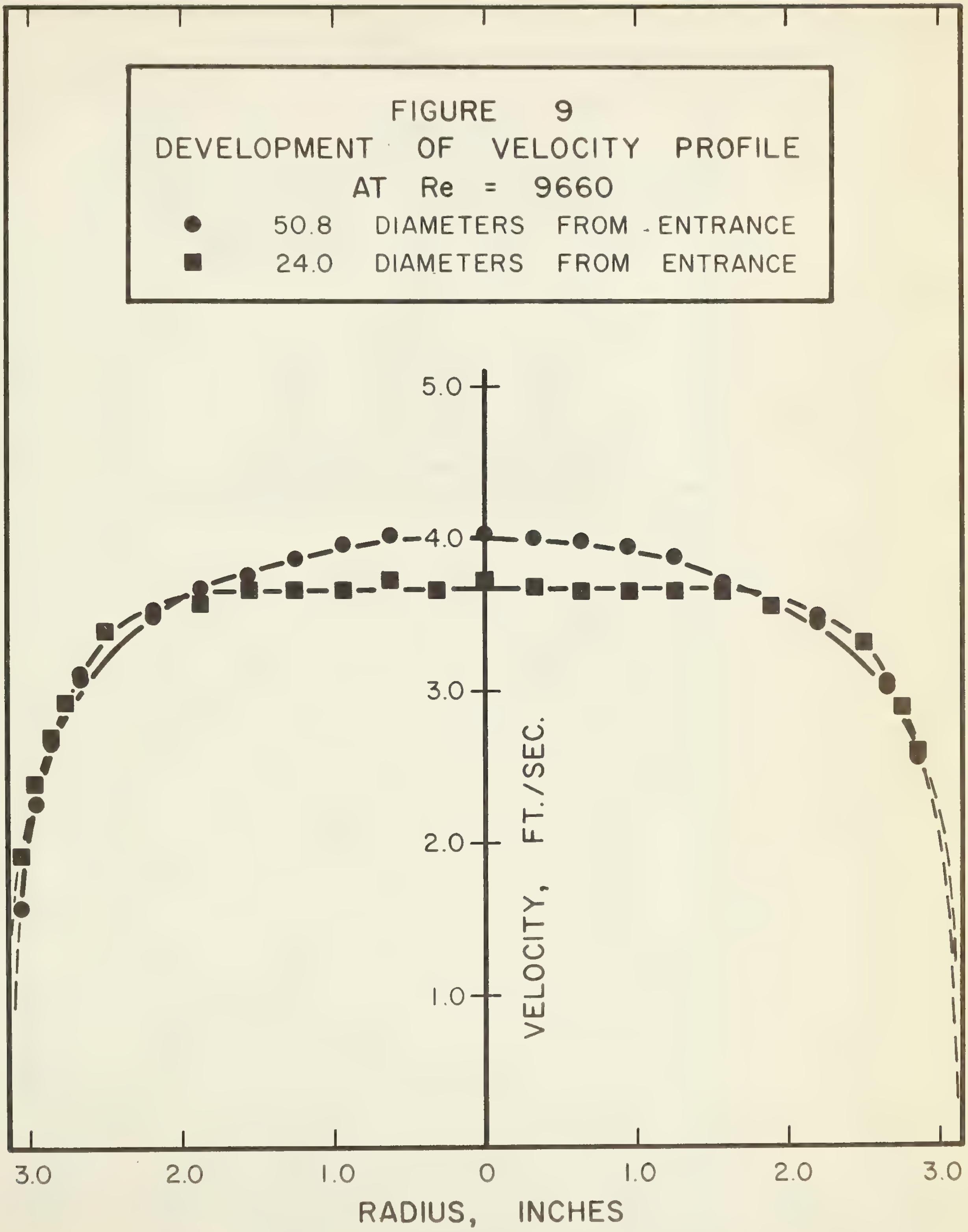

FIGURE 9
DEVELOPMENT OF VELOCITY PROFILE
AT Re = 9660

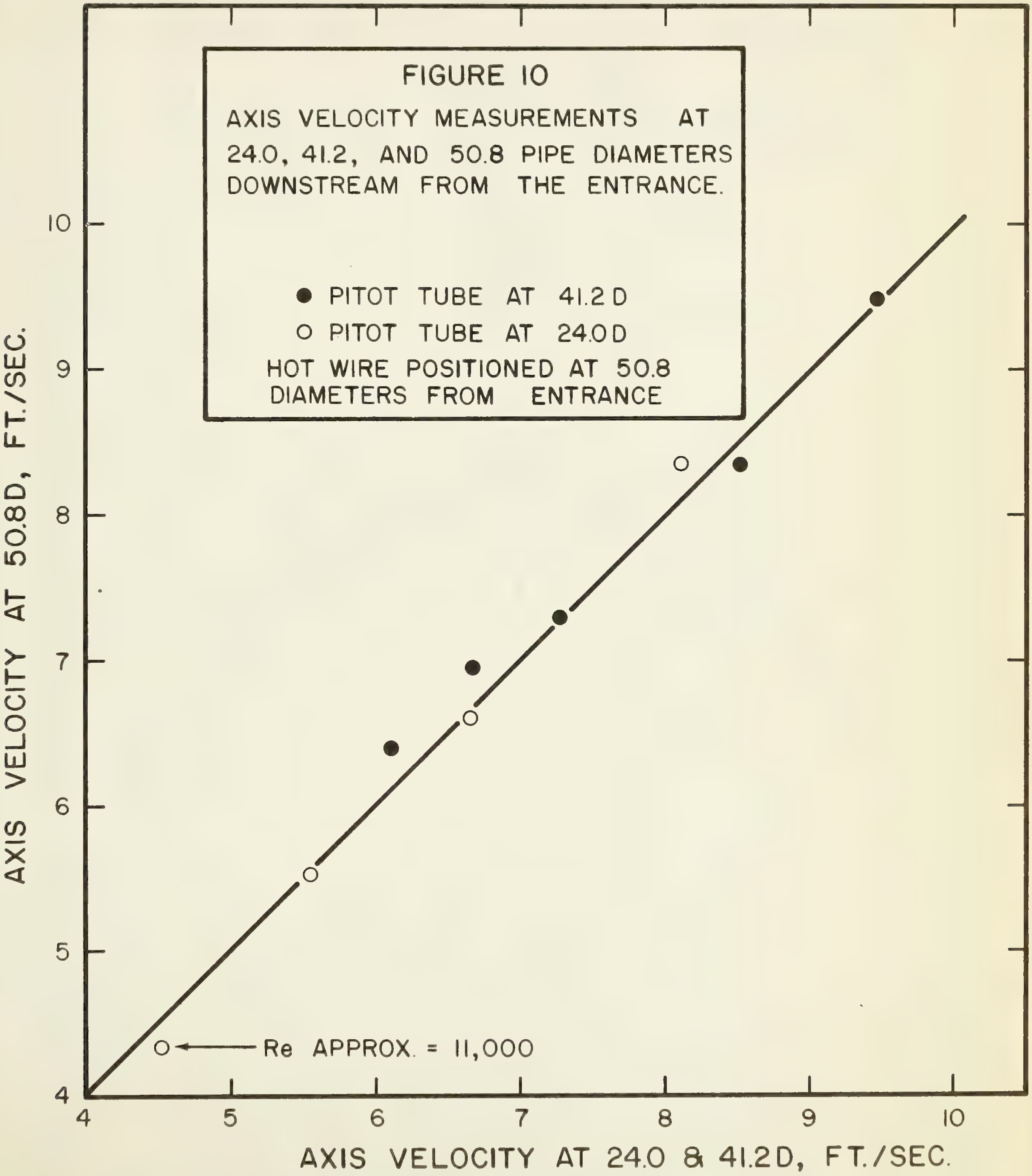

FIGURE 10

AXIS VELOCITY MEASUREMENTS AT 24.0, 41.2, AND 50.8 PIPE DIAMETERS DOWNSTREAM FROM THE ENTRANCE.

FIGURE 11
EXPERIMENTAL PROFILE COMPARED TO THEORETICAL FULLY DEVELOPED PROFILE FOR Re = 925

● MEASURED WITH HOT WIRE ANEMOMETER

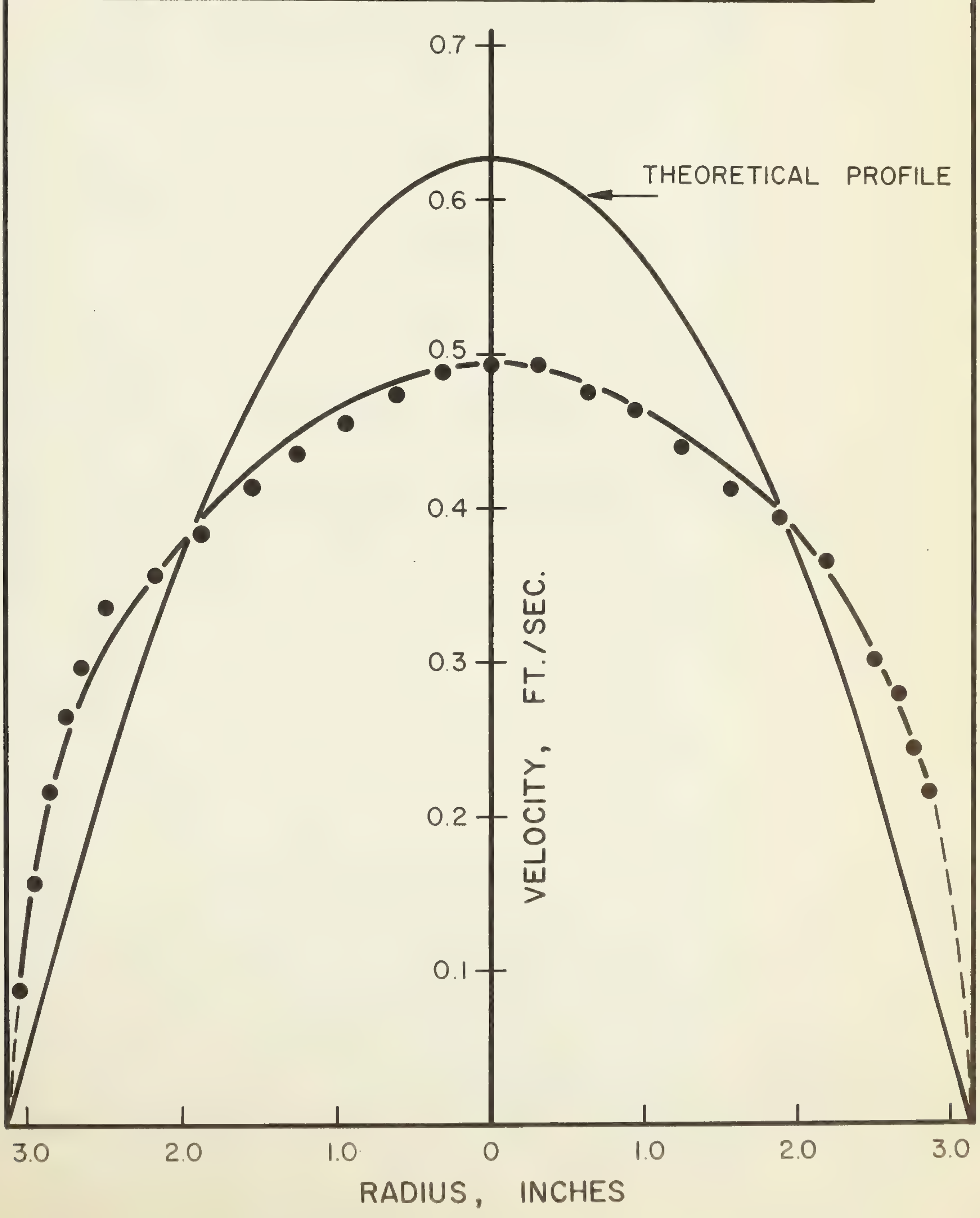

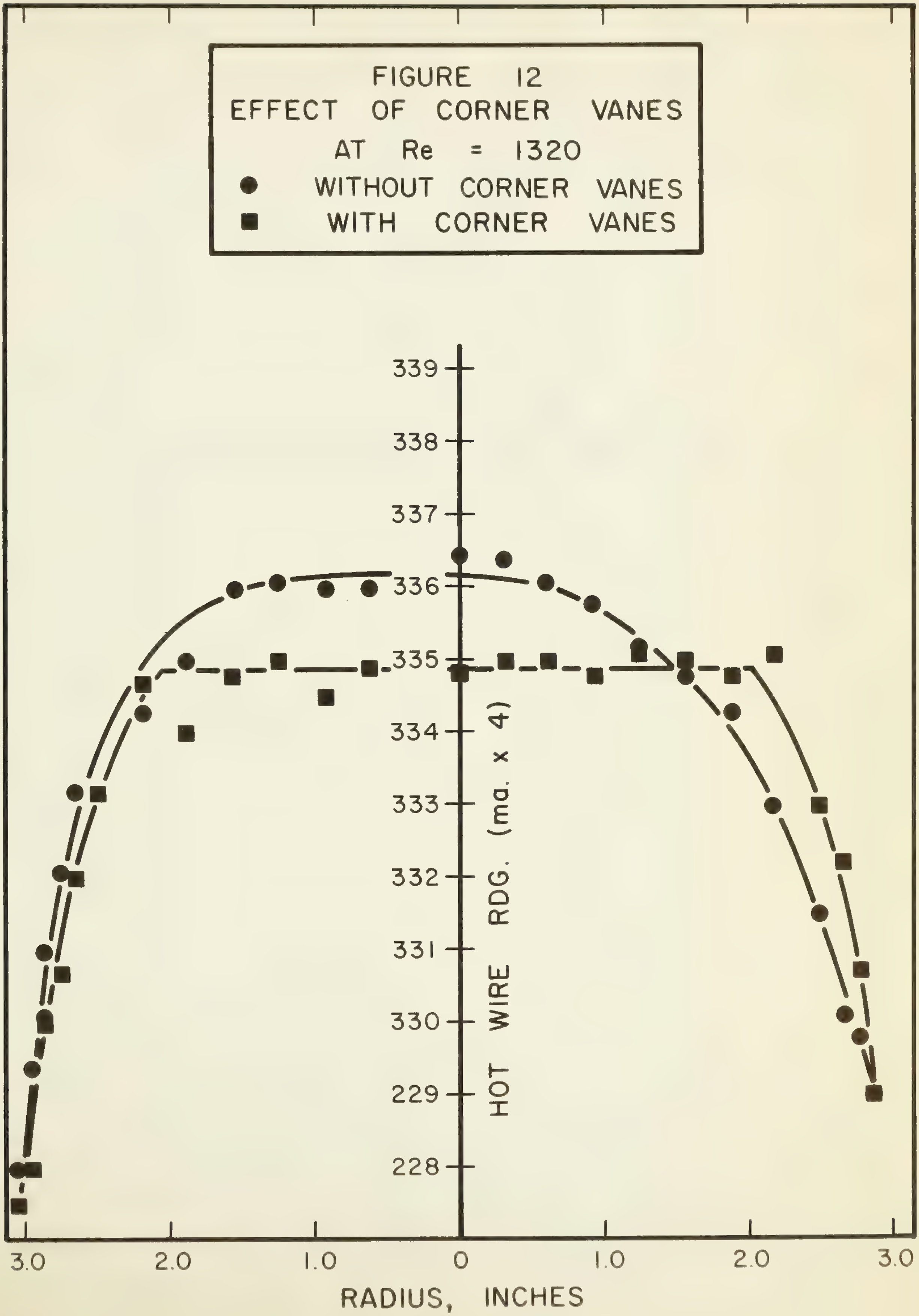

FIGURE 12
EFFECT OF CORNER VANES
AT Re = 1320

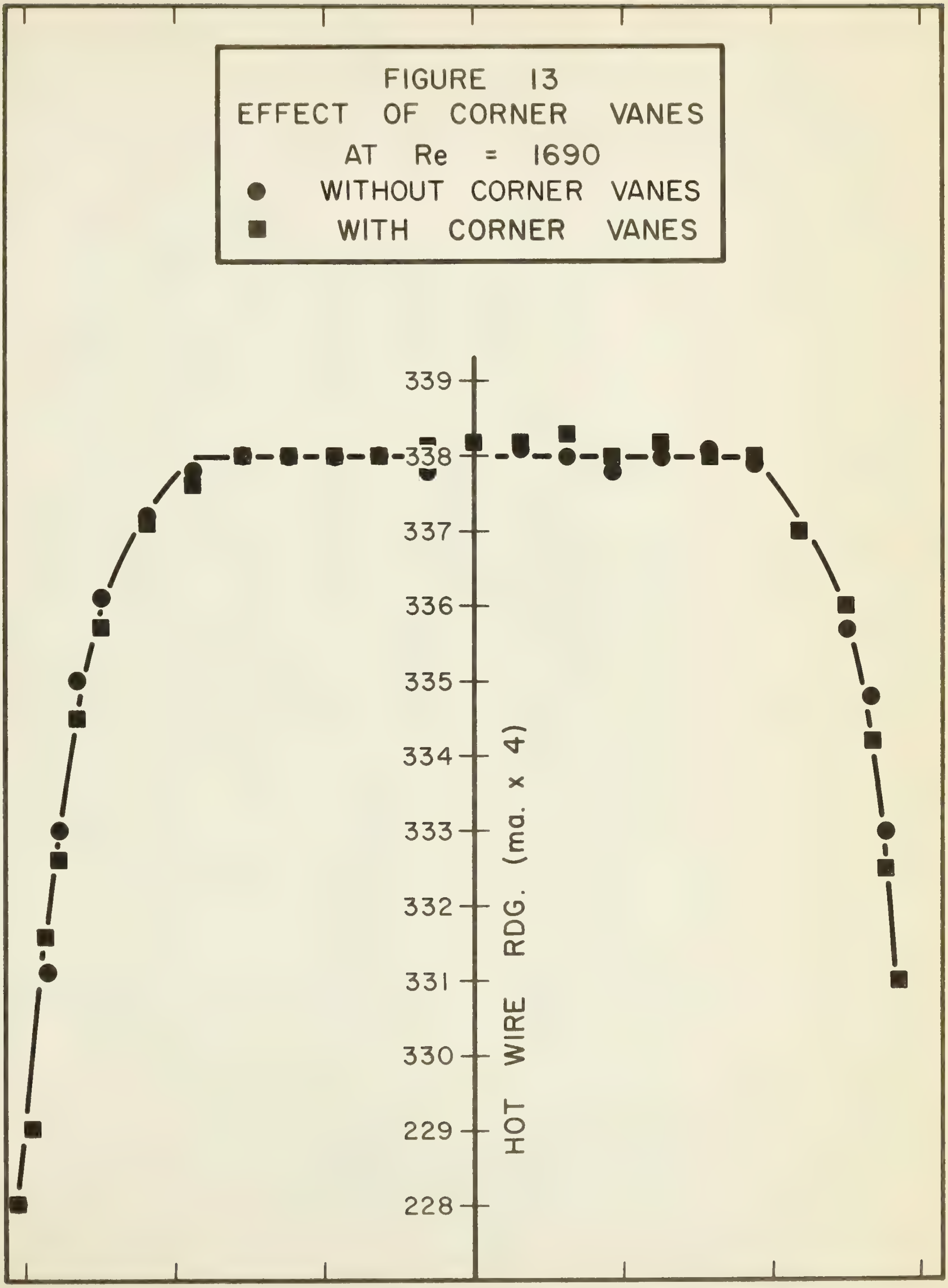

FIGURE 13
EFFECT OF CORNER VANES
AT Re = 1690

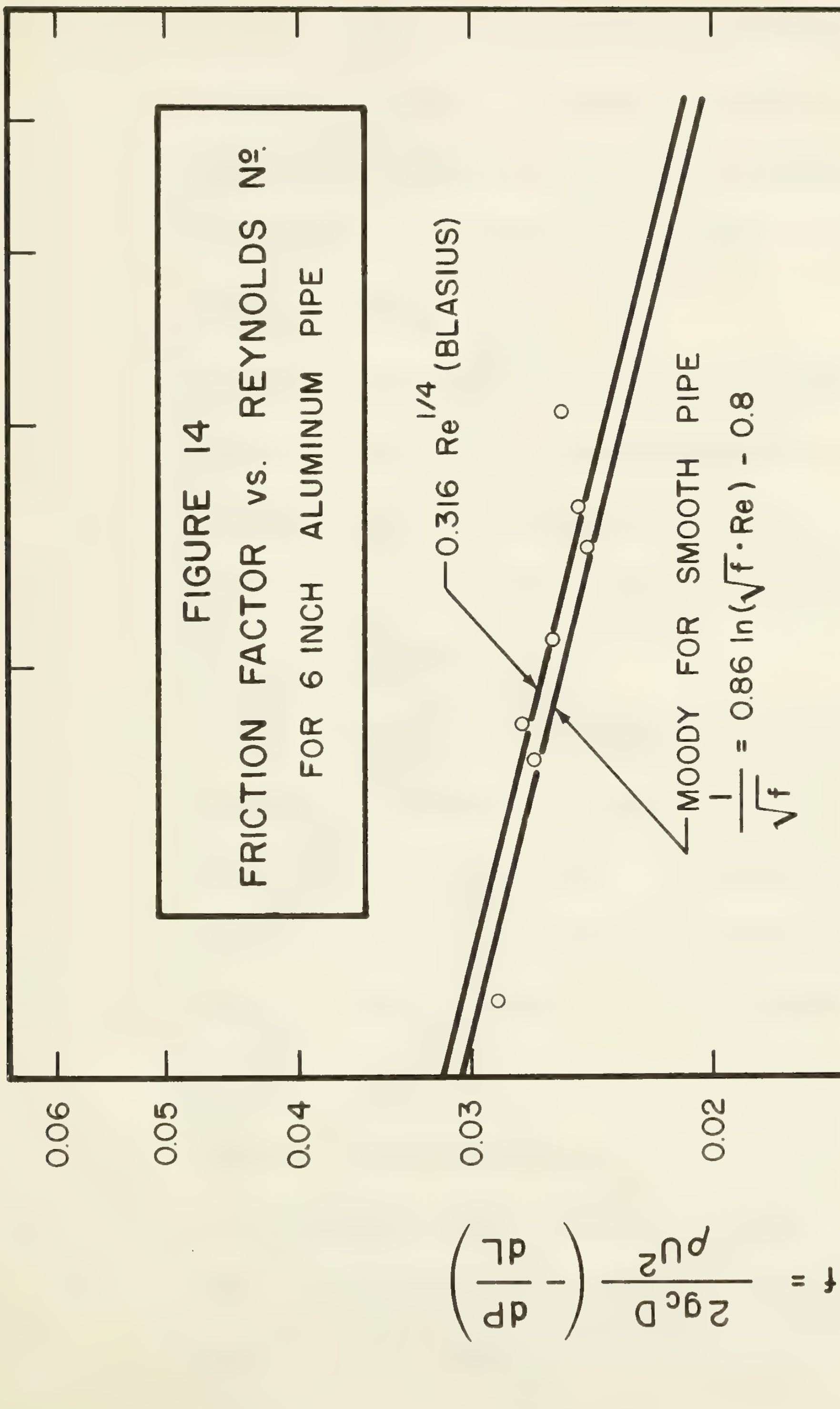

FIGURE 14
FRICTION FACTOR vs. REYNOLDS No.
FOR 6 INCH ALUMINUM PIPE

VI CONCLUSIONS AND RECOMMENDATIONS

1. At the section 50.8 diameters downstream from the entrance flow is fully developed in the Reynolds number range 11,430 to 30,800. The velocity profiles measured over this range compare with other published works and may be used for comparison with future profiles measured with gas-solids flow.
2. At Reynolds numbers below 11,000, down to a Reynolds number of 925, the profiles measured were not characteristic of fully developed ones and at these lower flow rates it may be expected that the boundary layer is still developing.
3. No transition in the shape of velocity profiles for laminar and turbulent flow could be determined for this system, since fully developed velocity profiles were not obtained over the complete range of Reynolds numbers investigated. A test section consisting of a smaller diameter pipe would have to be employed to observe the transition in profile shape between laminar and turbulent flow, since the pipe employed in this work can not be significantly lengthened.
4. Over the tube length 24.0 to 59.3 diameters, fully

developed flow was found to exist at Reynolds numbers greater than 11,000.

Pressure drop data taken in this range correlated within 5 per cent of the friction factor curves for smooth tubes as given by Blasius (2) and Moody (7). Accordingly, the use of these standard friction factor curves will enable reliable prediction of pressure drop in the tube.

5. The corner vanes that were used resulted in symmetrical velocity profiles at Reynolds numbers below 1,320 and since they are upstream from the point of solids entry it is felt that they should be employed for gas-solids flow measurement.
6. It is felt that further work to determine the exact starting length function of Reynolds number for a pipe with a diverging venturi entrance would prove to be significant and useful.

NOMENCLATURE

u	-	point velocity,	ft./sec.
u_m	-	maximum velocity,	ft./sec.
U	-	bulk velocity,	ft./sec.
u^+	-	dimensionless velocity,	dimensionless
u^*	-	friction velocity,	ft./sec.
y	-	distance from pipe wall,	inch
y^+	-	dimensionless distance from wall,	dimensionless
r	-	distance from pipe axis,	inch
r_w	-	radius of pipe,	inch
D	-	diameter of pipe,	inch
X	-	distance downstream from entrance of pipe,	ft.
L	-	pipe length,	ft.
P	-	pressure,	lb./ft.^{2}
T	-	temperature,	R.
τ_w	-	wall shear stress,	lb./ft.^{2}
I	-	hot wire current,	ma.
K	-	pitot tube constant,	dimensionless
Re	-	Reynolds number,	dimensionless
f	-	friction factor,	dimensionless
ν	-	kinematic viscosity,	ft.^{2}/sec.
Δh	-	pressure difference,	inch

ρ - density $\quad lb./ft.^3$

g_c - conversion constant $\quad \frac{lb._m}{lb._f} \; \frac{ft.}{sec.^2}$

$\frac{dP_f}{dL}$ - pressure gradient due to friction $\quad \frac{lb.}{ft.^3}$

BIBLIOGRAPHY

1. Bowers, B., "Flow of Gas-Solids Mixtures in a Verticle Circular Duct : I Calibration and Use of Velocity Measurement Devices", M.Sc. Thesis, University of Alberta, Incomplete.

2. Knudsen, J.G., and Katz, D.L., "Fluid Dynamics and Heat Transfer", McGraw-Hill Book Company, Inc., New York, N.Y. Ch. 7 and 9, 1958.

3. Rouse, H., "Fluid Mechanics for Hydraulic Engineers", McGraw-Hill Book Company, Inc., New York, N.Y., first edition, Ch. 12, 1938.

4. Rothfus, R.R., and Monrad, C.C., "Correlation of Turbulent Velocities for Tubes and Parallel Plates", Ind. and Eng. Chem., 47 : 1144, 1955.

5. Deissler, R.G., "Investigation of Turbulent Flow and Heat Transfer in Smooth Tubes, Including the Effects of Variable Fluid Properties", Trans. A.S.M.E., 73 : 101, 1951.

6. Campbell, J.S., and Brebner, A., "The Prediction of Flow Rates in Aluminum Pipe, Irrigation Tubing, and Fittings, and its Hydraulic Efficiency after Years of Service", Trans. Eng. Inst. Can., Vol.3, No.1, April, 1959.

7. Moody, L.F., "Friction Factors for Pipe Flow", Trans. A.S.M.E., 66 : 671, 1944.

8. Prandtl, L., and Tietjens, O.G., "Applied Hydro- and Aeromechanics", Dover Publications, Inc., New York, N.Y., Ch.3, 1957.

9. Deissler, R.G., "Turbulent Heat Transfer and Friction in the Entrance Regions of Smooth Passages", Trans. A.S.M.E., 77 : 1221, 1955.

10. Langhaar, H.L., "Steady Flow in the Transition Length of a Straight Tube", Trans. A.S.M.E., Vol.77, A-55, 1955.

11. Owen, E., and Johansen, F.C., "The Design of Pitot-Static Tubes", Aero. Res. Com. Reports and Memoranda, No. 981, 1925.

12. Brown, G.G. and Associates, "Unit Operations", John Wiley and Sons, Inc., New York, N.Y., 160, 1956.

13. Flow Corporation, "Selected Topics in Hot Wire Anemometer Theory", Bulletin 25.

APPENDICES

APPENDIX A

Calibration of the Equipment

1. Air Weight-Rate Recorder-Controller

The size of orifice plate for use in conjunction with the air weight-rate recorder-controller was calculated to be 1.544 inches, using the calibration data of the American Gas Association, Gas Measurement Committee Report No. 3.

An attempt was made to calibrate the controller by comparing the controller readings to the flow rates as calculated from pitot tube traverses. It was found, however, that the controller readings varied from 12 to 17 per cent too high. The flow rates as calculated from the pressure drop across the orifice and using the calibration data of the American Gas Association were within about 2 per cent of the controller readings. A pulsating flow through an orifice will result in a high indicated flow rate (12). This appears to be the case with this equipment since the positive displacement blower used for the experiments gave a pulsating air supply. The pulsations were dampened out in the 6-inch pipe but attempts to damp them out upstream from the orifice plate were unsuccessful. Table 32 shows the effect of blower speed on the flow rate. For these tests the controller was kept on automatic control and the blower speed was varied.

TABLE 32

EFFECT OF BLOWER SPEED ON FLOW RATE

- Pitot tube positioned in center of main flow pipe -

W.R.R.C. Setting ($ft.^3/min.$)	Blower Speed (rpm)	Pitot Tube Press. Diff. (in. alc.)
61	910	0.0107
61	985	0.0146
61	1050	0.0151
61	1120	0.0156
78	1120	0.0237
78	1190	0.0245
78	1255	0.0226
78	1325	0.0253

2. Pressure Recorder-Controller

The pressure recorder-controller was checked with a manometer and the results, as shown in Table 33, were found to be in good agreement.

TABLE 33

PRESSURE RECORDER-CONTROLLER CALIBRATION

P.R.C. Rdg. (psig)	Manometer Rdg. (cm.Hg.)	Manometer Rdg. (psig)
0.16	0.85	0.164
0.47	2.4	0.465
0.90	4.65	0.900
1.41	7.3	1.41
1.88	9.7	1.88
2.74	14.05	2.72

3. Temperature Recorder

The temperature recorder was checked with a calibrated mercury thermometer. The results are shown in Table 34.

TABLE 34

CHECK ON TEMPERATURE RECORDER

Remarks	Temp. Rec. (C.)	Temp. Rec. (F.)	Mercury Thermometer (F.)
ice water	0.5	33	33
room temp.	19	66	66
air flow	24.5	76	76

4. Hot Wire Anemometer

The hot wire probe was calibrated in the air velocity range of 5.5 to 13.0 ft./sec. using the pitot tube and micro-manometer as the primary measuring device. The pitot tube was first positioned at the center of the main flow pipe and readings were taken with the micro-manometer as the air flow rates were varied with the weight rate controller. The hot wire was then positioned in the center of the main flow pipe and the current readings were taken as the flow rates were reproduced by the weight rate controller.

Five calibration points in the lower velocity range (0.5 to 1.1 ft./sec.) were obtained by using a calibrated orifice. A 0.375 inch orifice was calibrated in place with a displacement meter (the displacement meter was calibrated with a gas-holder).

Hot wire traverses were then taken at 5 different flow rates. The centerline hot wire readings were used as the calibration points by assuming that the ratio of bulk velocity to centerline velocity was 0.80. The velocity profiles were then calculated using these calibration points. The ratios of bulk velocities to centerline velocities were calculated from these profiles and they were found to differ from the assumed value, 0.80. The calibration points were then adjusted using the calculated ratio of bulk velocity to centerline velocity and the profiles were recalculated. Table 35 shows the good agreement that was obtained between the flow rates as calculated from the orifice and by graphically integrating the velocity profiles obtained using the adjusted calibration points.

TABLE 35

FLOW RATES AS CALCULATED BY ORIFICE PLATE AND FROM HOT WIRE TRAVERSES

Traverse No.	Q (from hot wire trav.) (cu. ft./sec.)	Q (from orif. calc.) (cu. ft./sec.)
1	0.0709	0.0667
2	0.0951	0.0968
3	0.1178	0.1238
4	0.1636	0.1596
5	0.2063	0.2063

The calibration points from a lower value of 0.5 ft./sec. up to 9 ft./sec. lie on the straight line:

$$I^2 = 1094\,(u)^{\frac{1}{2}} + 6229$$

where, I = hot wire current, ma.

u = air velocity, ft./sec.

The general relationship between the hot wire current and the air velocity was obtained from the Flow Corporation Manual (13).

The hot wire probe was calibrated using the maximum allowable wire resistance ratio of 1.4. This resistance ratio gave the maximum resolution for air velocity measurement.

The experimental and calculated hot wire calibration data appear in Tables 27 and 28 of Appendix B. For a detailed description of the calibration of the hot wire probe, the reader is referred to Bowers' thesis (1).

APPENDIX B

Experimental and Calculated Data

- Velocity Calculations from Pitot Tube Measurements -

The standard equation that was used for velocity calculations from measurements made with the pitot tube is:

$$u = \sqrt{\frac{2g_c K \Delta P}{\rho}}$$

where u = air velocity, ft./sec.

ρ = air density, lb./ft.^{3}

K = pitot tube calibration constant, dimensionless

g_c = 32.17 lb.$_m$ ft./lb.$_f$ sec.^{2}

ΔP = difference between impact and static pressures, lb./ft.^{2}

The pitot tube calibration constant, K, was obtained by smoothing the calibration data of Ower and Johansen (11). The air density was calculated from the ideal gas law.

TABLE 1

PITOT TUBE TRAVERSE 1

W.R.R.C. - 43 ft.^{3}/min.
Bar. Press. - 70.12 cm. Hg.
Blower Speed - 910 rpm

Flowing Temp. - 18.5 C.
Room Temp. - 68 F.
Pt. of Measurement - 50.8 D. & 24.0 D.

	Probe Position (in.)	Δh (in.alc.)	u approx. ft./sec.	K	Δh x K (in.alc.)	u ft./sec.	ur ft. in./sec.
1a	2.97	0.0020	2.78	0.965	0.00193	2.73	8.11
	2.81	0.0030	3.41	0.970	0.00291	3.36	9.45
	2.50	0.0038	3.84	0.973	0.00370	3.79	9.48
	2.19	0.0044	4.13	0.976	0.00430	4.08	8.94
	1.87	0.0049	4.36	0.977	0.00479	4.30	8.05
	1.56	0.0053	4.53	0.978	0.00519	4.48	6.99
	1.25	0.0055	4.62	0.979	0.00538	4.56	5.70
	0.93	0.0058	4.74	0.980	0.00569	4.69	4.36
	0.62	0.0059	4.78	0.980	0.00579	4.73	2.93
	0.31	0.0061	4.86	0.981	0.00599	4.82	1.50
	0	0.0061	4.86	0.981	0.00599	4.82	0
1b	0.32	0.0061	4.86	0.981	0.00599	4.82	1.55
	0.63	0.0060	4.82	0.980	0.00589	4.78	3.01
	0.94	0.0057	4.70	0.980	0.00559	4.65	4.37
	1.25	0.0054	4.57	0.979	0.00529	4.53	5.66
	1.57	0.0052	4.49	0.978	0.00509	4.44	6.97
	1.88	0.0046	4.22	0.977	0.00450	4.18	7.86
	2.19	0.0043	4.08	0.976	0.00420	4.03	8.83
	2.51	0.0038	3.84	0.973	0.00370	3.79	9.51
	2.82	0.0030	3.41	0.970	0.00291	3.36	9.47
	2.98	0.0022	2.92	0.965	0.00212	2.87	8.55

$$T = (18.5 + 273)\ 1.8 = 525 \text{ R.}$$

$$P = 70.12 \times 14.7/76.0 = 13.57 \text{ psia}$$

$$\rho = 13.57 \times 29/10.72 \times 525 = 0.0698 \text{ lb./ft.}^3$$

$$u = (2g_c K\ P/\rho)^{\frac{1}{2}}$$

$$u = (3870 \times K \times \Delta h)^{\frac{1}{2}}$$

NOTE: 1a Measured 24.0 Pipe Diameters from Entrance
1b Measured 50.8 Pipe Diameters from Entrance

TABLE 2

PITOT TUBE TRAVERSE 2

W.R.R.C. - 61 ft.^{3}/min.
Bar. Press - 70.78 cm. Hg.
Blower Speed - 1050 rpm

Flowing Temp. - 21.5 C.
Room Temp. - 73 F.
Pt. of Measurement - 50.8 D.

Probe Position (in.)	Δh (in.alc.)	u approx. ft./sec.	K	Δh x K (in.alc.)	u ft./sec.	ur ft. in./sec.
2.97	0.0060	4.82	0.981	0.00589	4.77	14.18
2.81	0.0070	5.20	0.983	0.00688	5.16	14.51
2.50	0.0078	5.49	0.986	0.00770	5.46	13.67
2.19	0.0088	5.83	0.988	0.00869	5.80	12.70
1.87	0.0100	6.22	0.990	0.00990	6.19	11.58
1.56	0.0110	6.53	0.991	0.01090	6.50	10.14
1.25	0.0116	6.70	0.991	0.0115	6.67	8.34
0.93	0.0123	6.90	0.992	0.0122	6.88	6.40
0.62	0.0126	6.98	0.992	0.0125	6.96	4.31
0.31	0.0127	7.01	0.992	0.0126	6.98	2.16
0	0.0129	7.06	0.992	0.0128	7.04	0
0.32	0.0127	7.01	0.992	0.0126	6.98	2.23
0.63	0.0124	6.93	0.992	0.0123	6.90	4.35
0.94	0.0120	6.82	0.992	0.0119	6.79	6.38
1.25	0.0115	6.67	0.992	0.0114	6.64	8.36
1.57	0.0108	6.47	0.991	0.0107	6.44	10.06
1.88	0.0100	6.22	0.990	0.00990	6.19	11.62
2.19	0.0091	5.94	0.988	0.00899	5.90	13.00
2.51	0.0080	5.56	0.985	0.00790	5.53	13.88
2.82	0.0069	5.17	0.983	0.00678	5.12	14.44
2.98	0.0059	4.78	0.981	0.00580	4.74	14.12

TABLE 3

PITOT TUBE TRAVERSE 3

W.R.R.C. - 67 $ft.^3$/min.
Bar. Press. - 70.65 cm. Hg.
Blower Speed - 1050 rpm

Flowing Temp. - 21 C.
Room Temp. - 72 F.
Pt. of Measurement - 50.8 D.

Probe Position (in.)	Δh (in.alc.)	u approx. ft./sec.	K	$\Delta h \times K$ (in.alc.)	u ft./sec.	ur ft. in./sec.
2.97	0.0065	5.02	0.982	0.00638	4.98	14.8
2.81	0.0080	5.57	0.986	0.00789	5.53	15.5
2.50	0.0095	6.07	0.989	0.00940	6.04	15.1
2.19	0.0105	6.38	0.991	0.01041	6.36	13.9
1.87	0.0115	6.68	0.992	0.01140	6.65	12.4
1.56	0.0124	6.94	0.992	0.01230	6.91	10.8
1.25	0.0132	7.16	0.992	0.01309	7.12	8.9
0.93	0.0137	7.29	0.992	0.01360	7.26	6.8
0.62	0.0142	7.42	0.992	0.01409	7.39	4.6
0.31	0.0146	7.52	0.991	0.01448	7.50	2.3
0	0.0148	7.58	0.991	0.01468	7.54	0
0.32	0.0146	7.52	0.991	0.01448	7.50	2.4
0.63	0.0142	7.42	0.992	0.01409	7.39	4.6
0.94	0.0137	7.29	0.992	0.01360	7.26	6.8
1.25	0.0131	7.13	0.992	0.01291	7.08	8.9
1.57	0.0124	6.94	0.992	0.01230	6.91	10.9
1.88	0.0115	6.68	0.992	0.01140	6.65	12.5
2.19	0.0105	6.38	0.991	0.01041	6.36	13.9
2.51	0.0093	6.01	0.989	0.00919	5.97	15.0
2.82	0.0080	5.57	0.986	0.00789	5.53	15.6
2.98	0.0064	4.98	0.982	0.00629	4.94	14.7

TABLE 4

PITOT TUBE TRAVERSE 4

W.R.R.C. - 78 ft.^{3}/min.
Bar. Press. - 70.78 cm. Hg.
Blower Speed - 1050 rpm

Flowing Temp. - 23 C.
Room Temp. - 75 F.
Pt. of Measurement - 50.8 D.

Probe Position (in.)	Δh (in.alc.)	u approx. ft./sec.	K	Δh x K (in.alc.)	u ft./sec.	ur ft. in./sec.
2.97	0.0087	5.84	0.988	0.00859	5.78	17.2
2.81	0.0105	6.52	0.991	0.01041	6.37	17.9
2.50	0.0125	7.00	0.992	0.01240	6.94	17.3
2.19	0.0141	7.43	0.991	0.01398	7.38	16.2
1.87	0.0153	7.74	0.990	0.01516	7.68	14.4
1.56	0.0164	8.01	0.990	0.01623	7.95	12.4
1.25	0.0174	8.26	0.989	0.01720	8.18	10.2
0.93	0.0183	8.47	0.988	0.01809	8.39	7.8
0.62	0.0190	8.64	0.988	0.01878	8.55	5.3
0.31	0.0194	8.71	0.987	0.01917	8.64	2.7
0	0.0196	8.76	0.987	0.01935	8.68	0
0.32	0.0194	8.71	0.987	0.01917	8.64	2.8
0.63	0.0190	8.64	0.988	0.01878	8.55	5.4
0.94	0.0183	8.47	0.988	0.01809	8.39	7.9
1.25	0.0174	8.26	0.989	0.01720	8.18	10.2
1.57	0.0164	8.01	0.990	0.01623	7.95	12.5
1.88	0.0153	7.74	0.990	0.01516	7.68	14.4
2.19	0.0141	7.43	0.991	0.01398	7.38	16.2
2.51	0.0123	6.95	0.992	0.01220	6.89	17.3
2.82	0.0103	6.35	0.991	0.01021	6.30	17.8
2.98	0.0083	5.70	0.987	0.00820	5.65	16.8

TABLE 5

PITOT TUBE TRAVERSE 5

W.R.R.C. - 87 ft.^{3}/min.
Bar. Press. - 70.73 cm. Hg.
Blower Speed - 1325 rpm

Flowing Temp. - 22 C.
Room Temp. - 72 F.
Pt. of Measurement - 50.8 D.

Probe Position (in.)	Δh (in.alc.)	u approx. ft./sec.	K	Δh x K (in.alc.)	u ft./sec.	ur ft. in./sec.
2.97	0.0118	6.75	0.992	0.01170	6.74	20.0
2.81	0.0129	7.05	0.992	0.01280	7.05	19.8
2.50	0.0160	7.84	0.990	0.01583	7.84	19.6
2.19	0.0183	8.38	0.988	0.01808	8.38	18.3
1.87	0.0200	8.75	0.987	0.01975	8.75	16.4
1.56	0.0214	9.06	0.987	0.0211	9.06	14.1
1.25	0.0228	9.35	0.986	0.0225	9.34	11.7
0.93	0.0234	9.48	0.986	0.0231	9.47	8.81
0.62	0.0244	9.67	0.986	0.0241	9.67	6.00
0.31	0.0251	9.81	0.986	0.0248	9.80	3.04
0	0.0253	9.84	0.986	0.0250	9.84	0
0.32	0.0251	9.81	0.986	0.0248	9.80	3.14
0.63	0.0244	9.67	0.986	0.0241	9.67	6.10
0.94	0.0238	9.55	0.986	0.0235	9.55	8.98
1.25	0.0227	9.32	0.986	0.0224	9.32	11.6
1.57	0.0213	9.04	0.987	0.0210	9.04	14.2
1.88	0.0199	8.74	0.987	0.01965	8.74	16.4
2.19	0.0180	8.32	0.988	0.01780	8.31	18.2
2.51	0.0160	7.84	0.990	0.01583	7.84	19.7
2.82	0.0134	7.19	0.992	0.01330	7.18	20.2
2.98	0.0119	6.76	0.992	0.01180	6.77	20.2

TABLE 6

PITOT TUBE TRAVERSE 6

W.R.R.C. - 103 ft.^{3}/min.
Bar. Press. - 70.94 cm. Hg.
Blower Speed - 1350 rpm

Flowing Temp. - 23 C.
Room Temp. - 73 F.
Pt. of Measurement - 50.8 D.

Probe Position (in.)	Δh (in.alc.)	u approx. $\frac{\text{ft.}}{\text{sec.}}$	K	$\Delta h \times K$ (in.alc.)	u $\frac{\text{ft.}}{\text{sec.}}$	ur $\frac{\text{ft. in.}}{\text{sec.}}$
2.97	0.0127	7.06	0.992	0.01260	6.99	20.7
2.81	0.0158	7.87	0.990	0.01563	7.79	21.9
2.50	0.0192	8.68	0.987	0.01895	8.58	21.5
2.19	0.0218	9.25	0.986	0.0215	9.13	20.0
1.87	0.0241	9.72	0.986	0.0238	9.61	18.0
1.56	0.0261	10.11	0.936	0.0258	10.00	15.6
1.25	0.0276	10.40	0.987	0.0272	10.29	12.8
0.93	0.0288	10.62	0.988	0.0284	10.50	9.8
0.62	0.0297	10.80	0.989	0.0294	10.68	6.6
0.31	0.0303	10.90	0.990	0.0300	10.80	3.3
0	0.0306	10.95	0.990	0.0303	10.85	0
0.32	0.0303	10.90	0.990	0.0300	10.80	3.5
0.63	0.0297	10.80	0.989	0.0294	10.68	6.7
0.94	0.0288	10.62	0.988	0.0284	10.50	9.9
1.25	0.0276	10.40	0.987	0.0272	10.29	12.8
1.57	0.0261	10.11	0.986	0.0258	10.00	15.7
1.88	0.0241	9.72	0.986	0.0238	9.61	18.1
2.19	0.0218	9.25	0.986	0.0215	9.13	20.0
2.51	0.0192	8.68	0.987	0.01895	8.58	21.5
2.82	0.0156	7.82	0.990	0.01542	7.74	21.8
2.98	0.0127	7.06	0.992	0.01260	6.99	20.8

TABLE 7

PITOT TUBE TRAVERSE 7

W.R.R.C. - 116 ft.^{3}/min.	Flowing Temp. - 24 C.
Bar. Press. - 69.35 cm. Hg.	Room Temp. - 72 F.
Blower Speed - 1570 rpm	Pt. of Measurement - 50.8 D.

Probe Position (in.)	Δh (in.alc.)	u approx. ft./sec.	K	Δh x K (in.alc.)	u ft./sec.	ur ft. in./sec.
2.97	0.0197	8.82	0.987	0.01945	8.81	26.2
2.81	0.0228	9.49	0.986	0.0225	9.48	26.6
2.50	0.0272	10.36	0.987	0.0268	10.35	25.9
2.19	0.0305	10.99	0.990	0.0302	10.98	24.0
1.87	0.0331	11.47	0.993	0.0329	11.45	21.4
1.56	0.0358	11.92	0.995	0.0356	11.93	18.6
1.25	0.0380	12.30	0.996	0.0379	12.29	15.4
0.93	0.0393	12.51	0.997	0.0392	12.51	11.6
0.62	0.0406	12.71	0.998	0.0405	12.72	7.9
0.31	0.0421	12.96	0.999	0.0420	12.95	4.0
0	0.0426	13.02	0.999	0.0426	13.04	0
0.32	0.0419	12.95	0.999	0.0419	12.93	4.1
0.63	0.0410	12.78	0.998	0.0409	12.79	8.05
0.94	0.0396	12.57	0.997	0.0395	12.56	11.8
1.25	0.0381	12.31	0.996	0.0380	12.31	15.4
1.57	0.0356	11.90	0.995	0.0354	11.89	18.7
1.88	0.0333	11.50	0.993	0.0331	11.49	21.6
2.19	0.0303	10.97	0.990	0.0300	10.95	24.0
2.51	0.0270	10.32	0.987	0.0267	10.32	25.9
2.82	0.0227	9.46	0.986	0.0224	9.46	26.7
2.98	0.0193	8.74	0.987	0.01905	8.72	26.0

- Velocity Calculations from Hot Wire Anemometer Measurements -

The values of air velocity corresponding to the hot wire anemometer current reading were obtained from Figure 15, the calibration curve of the hot wire anemometer. Since the calibration curve has been adjusted to the conditions of air at a temperature of 530 R. and a pressure of 70.0 cm. Hg., the curve readings must be corrected for air temperatures and pressures different from 70 F. and 70.0 cm. Hg. The empirical method (13) of correcting the current reading for temperature variations is,

$$\text{Temperature Correction} = I_o^2 \left[(T_o - T)/T_o \right] 0.9$$

where, I_o = hot wire anemometer still air current reading, ma.

T_o = calibration air temp., R.

T = air temp., R.

The corrected value of the square of the current is then,

$$\text{Correct } I^2 = I^2 + \text{Temperature Correction}$$

where, I = hot wire anemometer current reading, ma.

The value of air velocity obtained from the calibration curve using this corrected value of the square of the current is corrected for pressure variations (13) by:

Correct $u = u \times P_o/P$

where, u = air velocity, ft./sec.

P_o = calibration air pressure, 70.0 cm. Hg.

P = air pressure, cm. Hg.

In all cases the temperature and pressure corrections are small.

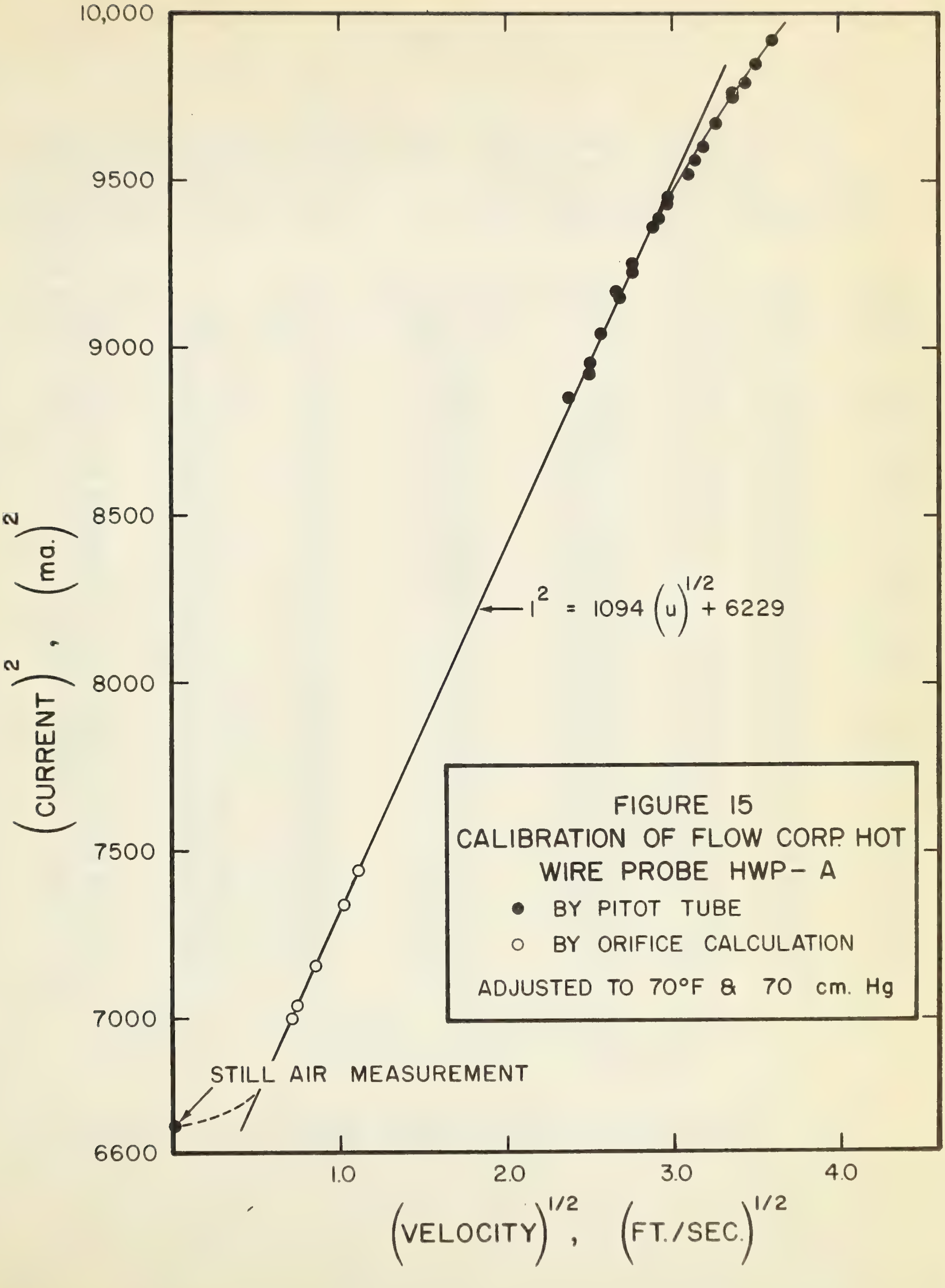

FIGURE 15
CALIBRATION OF FLOW CORP. HOT WIRE PROBE HWP- A

TABLE 8

HOT WIRE TRAVERSE 1

Orif. Press. Drop - 5.8 cm. H_2O
W.R.R.C. - 16 ft.^{3}/min. (l.c.)*
Orifice - 0.375"
Blower Speed - 910 rpm

Bar. Press. - 71.00 cm. Hg.
Flow Temp. - 25.0 C.
Hot Wire Still Air Rdg. - 326.7
Pt. of Measurement - 50.8 D.

Probe Position (in.)	I (ma.)	I^2 (ma.)^2	Corrected I^2 (ma.)^2	$\sqrt{\frac{P_u}{P_o}}$	P_u/P_o ft./sec.	u ft./sec.	ur ft. in./sec.
3.06	81.82	6695	6728	0.300	0.090	0.089	0.272
2.96	82.07	6735	6768	0.400	0.160	0.158	0.468
2.86	82.25	6765	6798	0.470	0.221	0.218	0.623
2.76	82.45	6798	6831	0.520	0.270	0.266	0.734
2.66	82.57	6818	6851	0.550	0.302	0.298	0.793
2.50	82.70	6840	6873	0.585	0.342	0.337	0.842
2.19	82.80	6856	6889	0.603	0.364	0.358	0.784
1.88	82.95	6880	6913	0.625	0.391	0.385	0.724
1.56	83.10	6905	6938	0.648	0.420	0.414	0.646
1.25	83.22	6925	6958	0.666	0.444	0.437	0.546
0.94	83.32	6942	6975	0.681	0.464	0.457	0.430
0.63	83.42	6958	6991	0.696	0.484	0.476	0.300
0.31	83.50	6971	7004	0.708	0.501	0.494	0.153
0.00	83.50	6971	7004	0.708	0.501	0.494	0
0.31	83.50	6971	7004	0.708	0.501	0.494	0.153
0.63	83.42	6958	6991	0.696	0.484	0.476	0.300
0.94	83.37	6950	6983	0.688	0.473	0.466	0.438
1.25	83.25	6930	6963	0.670	0.449	0.442	0.552
1.56	83.10	6905	6938	0.648	0.420	0.414	0.646
1.88	83.00	6889	6922	0.633	0.401	0.395	0.743
2.19	82.87	6866	6899	0.611	0.373	0.368	0.806
2.50	82.60	6823	6856	0.555	0.308	0.304	0.760
2.66	82.50	6806	6839	0.535	0.286	0.282	0.750
2.76	82.37	6785	6818	0.500	0.250	0.246	0.679
2.86	82.25	6765	6798	0.470	0.221	0.218	0.623

$$\text{Temperature Correction} = (81.75)^2 \frac{(540 - 537)}{540}\, 0.9 = 33 \text{ ma.}$$

* l.c. refers to linear chart used in flow controller

TABLE 9

HOT WIRE TRAVERSE 2

Orif. Pres. Drop - 12.0 cm. H_2O Bar. Press. - 69.82 cm. Hg.
W.R.R.C. - 32.5 ft.^{3}/min. (l.c.) Flow Temp. - 25.0 C.
Orifice - 0.375" Hot Wire Still Air Rdg. - 327.0
Blower Speed - 910 rpm Pt. of Measurement - 50.8 D

Probe Position (in.)	I (ma.)	I^2 (ma.)^2	Corrected I^2 (ma.)^2	$\sqrt{\frac{Pu}{P_o}}$	Pu/P_o ft./sec.	u ft./sec.	ur ft. in./sec.
3.06	81.87	6703	6736	0.330	0.109	0.109	0.333
2.96	82.00	6724	6757	0.380	0.144	0.144	0.426
2.86	82.50	6806	6839	0.535	0.286	0.287	0.821
2.76	82.67	6835	6868	0.575	0.331	0.332	0.916
2.66	83.00	6889	6922	0.633	0.401	0.402	1.069
2.50	83.30	6939	6972	0.679	0.461	0.462	1.155
2.19	83.67	7000	7033	0.734	0.539	0.540	1.183
1.88	83.50	6971	7004	0.708	0.501	0.502	0.944
1.56	83.70	7005	7038	0.739	0.546	0.547	0.853
1.25	83.75	7013	7046	0.747	0.558	0.559	0.699
0.94	83.62	6991	7024	0.726	0.527	0.528	0.496
0.63	83.72	7009	7042	0.743	0.552	0.553	0.348
0.31	83.75	7013	7046	0.747	0.558	0.559	0.173
0	83.70	7005	7038	0.739	0.546	0.547	0
0.31	83.75	7013	7046	0.747	0.558	0.559	0.173
0.63	83.75	7013	7046	0.747	0.558	0.559	0.352
0.94	83.70	7005	7038	0.739	0.546	0.547	0.514
1.25	83.77	7016	7049	0.749	0.561	0.562	0.702
1.56	83.75	7013	7046	0.747	0.558	0.559	0.872
1.88	83.70	7005	7038	0.739	0.546	0.547	1.028
2.19	83.77	7016	7049	0.749	0.561	0.562	1.231
2.50	83.25	6930	6963	0.670	0.449	0.450	1.125
2.66	83.05	6896	6929	0.639	0.408	0.409	1.088
2.76	82.67	6835	6868	0.575	0.331	0.332	0.916
2.86	82.25	6765	6798	0.470	0.221	0.222	0.635

Temperature Correction ≡ 33 ma.

TABLE 10

HOT WIRE TRAVERSE 3

Orif. Press. Drop - 19.6 cm. H_2O
W.R.R.C. - 52 ft.^{3}/min. (1.c.)
Orifice - 0.375"
Used Compressed Air

Bar. Press. - 69.96 cm. Hg.
Flow Temp. - 26.0 C.
Hot Wire Still Air Rdg. - 327.0
Pt. of Measurement - 50.8 D.

Probe Position (in.)	I (ma.)	I^2 $(ma.)^2$	Corrected I^2 $(ma.)^2$	$\sqrt{\frac{Pu}{P_o}}$	Pu/P_o ft./sec.	u ft./sec.	ur ft. in./sec.
3.06	82.00	6724	6735	0.330	0.109	0.109	0.333
2.96	82.25	6765	6776	0.425	0.181	0.181	0.536
2.86	82.75	6848	6859	0.560	0.314	0.314	0.898
2.76	83.15	6913	6924	0.635	0.403	0.403	1.112
2.66	83.62	6991	7002	0.706	0.498	0.498	1.325
2.50	83.92	7043	7054	0.754	0.568	0.568	1.420
2.19	84.27	7101	7112	0.806	0.650	0.650	1.423
1.88	84.40	7123	7134	0.826	0.682	0.682	1.282
1.56	84.50	7140	7151	0.842	0.709	0.709	1.106
1.25	84.50	7140	7151	0.842	0.709	0.709	0.886
0.94	84.50	7140	7151	0.842	0.709	0.709	0.666
0.63	84.50	7140	7151	0.842	0.709	0.709	0.447
0.31	84.52	7143	7154	0.845	0.714	0.714	0.221
0	84.55	7148	7159	0.850	0.722	0.722	0
0.31	84.57	7151	7162	0.852	0.726	0.726	0.225
0.63	84.57	7151	7162	0.852	0.726	0.726	0.457
0.94	84.50	7140	7151	0.842	0.709	0.709	0.666
1.25	84.55	7148	7151	0.842	0.709	0.709	0.886
1.56	84.50	7140	7151	0.842	0.709	0.709	1.106
1.88	84.50	7140	7151	0.842	0.709	0.709	1.333
2.19	84.25	7099	7110	0.805	0.648	0.648	1.419
2.50	84.00	7056	7067	0.766	0.587	0.587	1.467
2.66	83.55	6980	6991	0.696	0.484	0.484	1.287
2.76	83.12	6909	6920	0.631	0.398	0.398	1.098
2.86	82.75	6848	6849	0.550	0.302	0.302	0.864

Temperature Correction = 11 ma.

TABLE 11

HOT WIRE TRAVERSE 4

Orif. Press. Drop - 33.1 cm. H_2O
W.R.R.C. - 90 $ft.^3/min.$ (l.c.)
Orifice - 0.375"
Blower Speed - 910 rpm

Bar. Press. - 71.00 cm. Hg.
Flow Temp. - 26.0 C.
Hot Wire Still Air Rdg. - 327.0
Pt. of Measurement - 50.8 D.

Probe Position (in.)	I (ma.)	I^2 $(ma.)^2$	Corrected I^2 $(ma.)^2$	$\sqrt{\frac{Pu}{P_o}}$	Pu/P_o $\frac{ft.}{sec.}$	u $\frac{ft.}{sec.}$	ur $\frac{ft.\ in.}{sec.}$
3.06	82.37	6785	6796	0.460	0.212	0.209	0.639
2.96	82.92	6875	6886	0.600	0.360	0.355	1.051
2.86	83.32	6941	6952	0.660	0.436	0.430	1.230
2.76	83.75	7013	7024	0.726	0.527	0.520	1.435
2.66	84.20	7090	7101	0.797	0.635	0.625	1.662
2.50	84.62	7160	7171	0.860	0.740	0.730	1.825
2.19	85.12	7245	7256	0.937	0.878	0.865	1.894
1.88	85.42	7297	7308	0.985	0.970	0.955	1.795
1.56	85.62	7330	7341	1.018	1.036	1.020	1.591
1.25	85.62	7330	7341	1.018	1.036	1.020	1.275
0.94	85.62	7330	7341	1.018	1.036	1.020	0.959
0.63	85.62	7330	7341	1.018	1.036	1.020	0.643
0.31	85.62	7330	7341	1.018	1.036	1.020	0.316
0	85.62	7330	7341	1.018	1.036	1.020	0
0.31	85.62	7330	7341	1.018	1.036	1.020	0.316
0.63	85.62	7330	7341	1.018	1.036	1.020	0.643
0.94	85.62	7330	7341	1.018	1.036	1.020	0.959
1.25	85.62	7330	7341	1.018	1.036	1.020	1.275
1.56	85.57	7321	7332	1.009	1.018	1.002	1.563
1.88	85.50	7310	7321	0.998	0.996	0.982	1.846
2.19	85.25	7267	7278	0.959	0.920	0.906	1.984
2.50	84.70	7174	7185	0.874	0.764	0.753	1.882
2.66	84.10	7073	7084	0.781	0.610	0.601	1.599
2.76	83.80	7021	7032	0.733	0.537	0.529	1.460
2.86	83.25	6931	6941	0.650	0.422	0.415	1.187

Temperature Correction ≅ 11 ma.

TABLE 12

HOT WIRE TRAVERSE 5

Orif. Press. Drop - 55.0 cm. H_2O
W.R.R.C. - 148 ft.^{3}/min. (l.c.)
Orifice - 0.375"
Blower Speed - 910 rpm

Bar. Press. - 71.00 cm. Hg.
Flow Temp. - 27.5 C.
Hot Wire Still Air Rdg. - 327.0
Pt. of Measurement - 50.8 D.

Probe Position (in.)	I (ma.)	I^2 (ma.)^2	Corrected I^2 (ma.)^2	$\sqrt{\frac{P_u}{P_o}}$	P_u/P_o ft./sec.	u ft./sec.	ur ft. in./sec.
3.06	83.12	6909	6898	0.611	0.373	0.368	1.126
2.96	84.07	7069	7058	0.757	0.573	0.565	1.672
2.86	84.55	7149	7138	0.830	0.689	0.679	1.942
2.76	84.90	7208	7197	0.884	0.781	0.770	2.125
2.66	85.25	7267	7256	0.938	0.880	0.867	2.306
2.50	85.50	7310	7249	0.977	0.954	0.940	2.350
2.19	86.07	7409	7398	1.068	1.140	1.123	2.459
1.88	86.20	7430	7419	1.087	1.182	1.167	2.194
1.56	86.25	7439	7428	1.094	1.196	1.179	1.839
1.25	86.30	7448	7437	1.102	1.215	1.198	1.497
0.94	86.25	7439	7428	1.094	1.196	1.179	1.108
0.63	86.30	7448	7437	1.102	1.215	1.198	0.755
0.31	86.25	7439	7428	1.094	1.196	1.179	0.365
0	86.32	7451	7440	1.106	1.222	1.205	0
0.31	86.25	7439	7428	1.094	1.196	1.179	0.365
0.63	86.25	7439	7428	1.094	1.196	1.179	0.743
0.94	86.32	7451	7440	1.106	1.222	1.205	1.133
1.25	86.25	7439	7428	1.094	1.196	1.179	1.474
1.56	86.25	7439	7428	1.094	1.196	1.179	1.839
1.88	86.15	7421	7410	1.080	1.166	1.149	2.160
2.19	85.87	7373	7362	1.035	1.072	1.059	2.319
2.50	85.62	7330	7319	0.995	0.990	0.975	2.437
2.66	85.25	7267	7256	0.938	0.880	0.867	2.306
2.76	85.05	7233	7222	0.907	0.823	0.811	2.238
2.86	84.67	7169	7158	0.849	0.721	0.711	2.033

Temperature Correction ≅ -11 ma.

TABLE 13

HOT WIRE TRAVERSE 6

W.R.R.C. - 82 ft.^{3}/min. (l.c.)
Orifice - 0.75"
Blower Speed - 910 rpm

Bar. Press. - 70.82 cm. Hg.
Flow Temp. - 25.0 C.
Hot Wire Still Air Rdg. - 327.0
Pt. of Measurement - 50.8 D.

Probe Position (in.)	I (ma.)	I^2 (ma.)^2	Corrected I^2 (ma.)^2	$\sqrt{\frac{Pu}{P_o}}$	Pu/P_o $\frac{ft.}{sec.}$	u $\frac{ft.}{sec.}$	ur $\frac{ft.\ in.}{sec.}$
3.06	84.55	7149	7182	0.870	0.757	0.749	2.291
2.96	85.50	7310	7343	1.019	1.038	1.026	3.037
2.86	86.25	7439	7472	1.137	1.292	1.280	3.661
2.76	86.82	7537	7570	1.226	1.502	1.486	4.101
2.66	87.32	7625	7658	1.305	1.702	1.685	4.482
2.50	87.82	7711	7744	1.384	1.912	1.891	4.727
2.19	88.12	7765	7798	1.433	2.052	2.030	4.446
1.88	88.50	7832	7865	1.493	2.229	2.205	4.145
1.56	88.60	7850	7883	1.511	2.282	2.260	3.526
1.25	88.77	7880	7913	1.539	2.370	2.340	2.925
0.94	88.77	7880	7913	1.539	2.370	2.340	2.200
0.63	88.77	7880	7913	1.539	2.370	2.340	1.474
0.31	88.77	7880	7913	1.539	2.370	2.340	0.725
0	88.80	7885	7918	1.543	2.380	2.350	0
0.31	88.77	7880	7913	1.539	2.370	2.340	0.725
0.63	88.77	7880	7913	1.539	2.370	2.340	1.474
0.94	88.77	7880	7913	1.539	2.370	2.340	2.200
1.25	88.75	7877	7910	1.537	2.363	2.335	2.919
1.56	88.62	7853	7886	1.512	2.285	2.260	3.526
1.88	88.47	7828	7861	1.490	2.220	2.195	4.127
2.19	88.25	7789	7822	1.456	2.120	2.100	4.599
2.50	87.75	7700	7733	1.373	1.885	1.865	4.662
2.66	87.40	7639	7672	1.319	1.740	1.720	4.575
2.76	86.95	7560	7593	1.246	1.552	1.535	4.237
2.86	86.32	7451	7484	1.146	1.312	1.298	3.712

Temperature Correction ≅ -33 ma.

TABLE 14

HOT WIRE TRAVERSE 7

W.R.R.C. - 31 ft.^{3}/min.	Bar. Press. - 70.82 cm. Hg.
Orifice - 1.544"	Flow Temp. - 24.0 C.
Blower Speed - 910 rpm	Hot Wire Still Air Rdg. - 327.0
	Pt. of Measurement - 50.8 D.

Probe Position (in.)	I (ma.)	I^2 (ma.)^2	Corrected I^2 (ma.)^2	$\sqrt{\frac{Pu}{P_o}}$	Pu/P_o $\frac{ft.}{sec.}$	u $\frac{ft.}{sec.}$	ur $\frac{ft. in.}{sec.}$
3.06	86.87	7547	7603	1.255	1.575	1.560	4.774
2.96	88.45	7823	7879	1.508	2.272	2.245	6.645
2.86	89.22	7960	8016	1.631	2.660	2.63	7.522
2.76	89.75	8055	8111	1.720	2.960	2.92	8.059
2.66	90.10	8117	8173	1.775	3.150	3.12	8.299
2.50	90.50	8190	8246	1.840	3.387	3.35	8.375
2.19	90.75	8235	8291	1.884	3.550	3.51	7.687
1.88	91.02	8285	8341	1.928	3.717	3.67	6.900
1.56	91.17	8311	8367	1.950	3.805	3.76	5.866
1.25	91.30	8335	8391	1.975	3.900	3.86	4.825
0.94	91.45	8363	8419	2.000	4.000	3.96	3.722
0.63	91.55	8381	8437	2.016	4.065	4.01	2.526
0.31	91.57	8386	8442	2.020	4.080	4.03	1.249
0	91.57	8386	8442	2.020	4.080	4.03	0
0.31	91.52	8376	8432	2.012	4.050	4.00	1.240
0.63	91.50	8372	8428	2.006	4.025	3.98	2.507
0.94	91.42	8358	8414	1.997	3.990	3.94	3.704
1.25	91.32	8340	8396	1.980	3.920	3.88	4.850
1.56	91.07	8293	8349	1.936	3.750	3.71	5.788
1.88	90.92	8267	8323	1.910	3.650	3.61	6.787
2.19	90.72	8230	8286	1.878	3.527	3.49	7.643
2.50	90.37	8167	8223	1.821	3.317	3.28	8.200
2.66	90.00	8100	8156	1.759	3.092	3.06	8.140
2.76	89.62	8031	8087	1.697	2.880	2.85	7.866
2.86	89.10	7939	7995	1.611	2.595	2.56	7.322

Temperature Correction ≅ 56 ma.

TABLE 15

HOT WIRE TRAVERSE 7a

W.R.R.C. - 31 ft.^{3}/min.
Orifice - 1.544"
Blower Speed - 910 rpm

Bar. Press. - 71.48 cm. Hg.
Flow Temp. - 24.0 C.
Hot Wire Still Air Rdg. - 326.7
Pt. of Measurement - 24.0 D.

Probe Position (in.)	I (ma.)	I^2 (ma.)^2	Corrected I^2 (ma.)^2	$\sqrt{\frac{Pu}{P_o}}$	Pu/P_o $\frac{\text{ft.}}{\text{sec.}}$	u $\frac{\text{ft.}}{\text{sec.}}$
3.06	87.50	7657	7713	1.357	1.84	1.81
2.96	88.75	7877	7933	1.558	2.42	2.38
2.86	89.30	7975	8031	1.648	2.72	2.67
2.76	89.75	8055	8111	1.721	2.96	2.91
2.66	90.05	8109	8165	1.769	3.13	3.07
2.50	90.55	8200	8256	1.852	3.43	3.37
2.19	90.75	8235	8291	1.885	3.55	3.48
1.88	90.87	8259	8315	1.906	3.63	3.56
1.56	91.05	8290	8346	1.932	3.73	3.66
1.25	91.00	8281	8337	1.928	3.72	3.65
0.94	91.00	8281	8337	1.928	3.72	3.65
0.63	91.12	8303	8359	1.946	3.79	3.72
0.31	91.05	8290	8346	1.932	3.73	3.66
0	91.10	8300	8356	1.944	3.78	3.71
0.31	91.07	8293	8349	1.937	3.75	3.68
0.63	91.00	8281	8337	1.928	3.72	3.65
0.94	91.00	8281	8337	1.928	3.72	3.65
1.25	91.00	8281	8337	1.928	3.72	3.65
1.56	91.02	8285	8341	1.930	3.72	3.65
1.88	90.75	8235	8291	1.885	3.55	3.48
2.19	90.68	8223	8279	1.872	3.50	3.44
2.50	90.50	8190	8246	1.840	3.38	3.32
2.66	89.92	8085	8141	1.749	3.06	3.01
2.76	89.70	8045	8101	1.711	2.93	2.88
2.86	89.18	7953	8009	1.627	2.65	2.60

Temperature Correction = 56 ma.

TABLE 16

PLOTTING DATA FOR UNIVERSAL VELOCITY DISTRIBUTION 1

Re = 11,430
f = 0.0305•

u* = 0.237 ft./sec.
U = 3.84 ft./sec.

y (ft.)	u (ft./sec.)	y^+	u^+
0.0133	2.73	18.0	11.52
0.0267	3.36	36.1	14.18
0.0525	3.79	71.0	15.99
0.0784	4.08	106	17.21
0.1050	4.30	142	18.14
0.1309	4.48	177	18.90
0.1567	4.56	212	19.24
0.1833	4.69	248	19.79
0.2092	4.73	283	19.96
0.2350	4.82	318	20.34
0.2342	4.82	316	20.34
0.2083	4.78	281	20.17
0.1826	4.65	247	19.62
0.1567	4.53	212	19.11
0.1300	4.44	176	18.73
0.1042	4.18	141	17.63
0.0784	4.03	106	17.00
0.0516	3.79	69.8	15.99
0.0258	3.36	34.9	14.18
0.0133	2.87	18.0	12.11

$\sqrt{f/8} = 0.0618$

$u^* = \sqrt{f/8}\ U$

$= 0.237$ ft./sec.

$u^+ = U/u^*$

$\nu = 1.755 \times 10^{-4}$ ft.²/sec.••

$u^*/\nu = 1.351 \times 10^{3}$/ft.

$y^+ = y(u^*/\nu)$

- Blasius friction factor (2)

•• Perry, J.H., "Chemical Engineers Handbook," McGraw-Hill Book Company, Inc., New York, N.Y., third edition, 370, 1950.

TABLE 17

PLOTTING DATA FOR UNIVERSAL VELOCITY DISTRIBUTION 2

Re = 17,190
f = 0.0276

u* = 0.338 ft./sec.
U = 5.75 ft./sec.

y (ft.)	u (ft./sec.)	y^+	u^+
0.0133	4.77	25.6	14.11
0.0267	5.16	51.4	15.26
0.0525	5.46	101	16.15
0.0784	5.80	151	17.16
0.1050	6.19	202	18.31
0.1309	6.50	252	19.23
0.1567	6.67	302	19.73
0.1833	6.88	353	20.35
0.2092	6.96	403	20.59
0.2350	6.98	453	20.65
0.2342	6.98	451	20.65
0.2083	6.90	401	20.41
0.1826	6.79	352	20.08
0.1567	6.64	302	19.64
0.1300	6.44	250	19.05
0.1042	6.19	201	18.31
0.0784	5.90	151	17.45
0.0516	5.53	99.5	16.36
0.0258	5.12	49.7	15.14
0.0133	4.74	25.6	14.02

TABLE 18

PLOTTING DATA FOR UNIVERSAL VELOCITY DISTRIBUTION 3

Re = 18,250
f = 0.0271

u^* = 0.357 ft./sec.
U = 6.13 ft./sec.

y (ft.)	u (ft./sec.)	y^+	u^+
0.0133	4.98	27.0	13.95
0.0267	5.53	54.3	15.49
0.0525	6.04	107	16.92
0.0784	6.36	160	17.81
0.1050	6.65	214	18.63
0.1309	6.91	266	19.35
0.1567	7.12	319	19.94
0.1833	7.26	373	20.33
0.2092	7.39	426	20.70
0.2350	7.50	478	21.01
0.2342	7.50	476	21.01
0.2083	7.39	424	20.70
0.1826	7.26	371	20.34
0.1567	7.08	319	19.83
0.1300	6.91	264	19.35
0.1042	6.65	212	18.63
0.0784	6.36	159	17.81
0.0516	5.97	105	16.72
0.0258	5.53	52.5	15.49
0.0133	4.94	27.1	13.84

TABLE 19

PLOTTING DATA FOR UNIVERSAL VELOCITY DISTRIBUTION 4

Re = 21,000
f = 0.0262

u^* = 0.406 ft./sec.
U = 7.09 ft./sec.

y (ft.)	u (ft./sec.)	y^+	u^+
0.0133	5.78	30.8	14.24
0.0267	6.37	61.8	15.69
0.0525	6.94	121	17.09
0.0784	7.38	181	18.18
0.1050	7.68	243	18.91
0.1309	7.95	303	19.58
0.1567	8.18	362	20.14
0.1833	8.39	424	20.66
0.2092	8.55	484	21.06
0.2350	8.64	544	21.28
0.2342	8.64	542	21.28
0.2083	8.55	482	21.06
0.1826	8.39	422	20.66
0.1567	8.18	362	20.15
0.1300	7.95	301	19.58
0.1042	7.68	241	18.92
0.0784	7.38	181	18.18
0.0516	6.89	119	16.97
0.0258	6.30	59.7	15.52
0.1033	5.65	30.8	13.92

TABLE 20

PLOTTING DATA FOR UNIVERSAL VELOCITY DISTRIBUTION 5

Re = 24,000

f = 0.0254

u* = 0.456 ft./sec.

U = 8.06 ft./sec.

y (ft.)	u (ft./sec.)	y^+	u^+
0.0133	6.74	34.6	14.78
0.0267	7.05	69.4	15.46
0.0525	7.84	137	17.19
0.0784	8.38	204	18.38
0.1050	8.75	273	19.19
0.1309	9.06	340	19.87
0.1567	9.34	407	20.48
0.1833	9.47	477	20.77
0.2092	9.67	544	21.21
0.2350	9.80	611	21.49
0.2342	9.80	609	21.49
0.2083	9.67	542	21.21
0.1826	9.55	475	20.94
0.1567	9.32	407	20.44
0.1300	9.04	338	19.82
0.1042	8.74	271	19.17
0.0784	8.31	204	18.22
0.0516	7.84	134	17.19
0.0258	7.18	67.1	15.72
0.0133	6.77	34.6	14.85

TABLE 21

PLOTTING DATA FOR UNIVERSAL VELOCITY DISTRIBUTION 6

Re = 26,200

f = 0.0249

u* = 0.492 ft./sec.

U = 8.83 ft./sec.

y (ft.)	u (ft./sec.)	y^+	u^+
0.0133	7.06	37.3	14.35
0.0267	7.87	75.0	16.00
0.0525	8.68	147	17.64
0.0784	9.25	220	18.80
0.1050	9.72	295	19.76
0.1309	10.11	367	20.55
0.1567	10.40	440	21.14
0.1833	10.62	515	21.59
0.2092	10.80	587	21.95
0.2350	10.90	660	22.15
0.2342	10.90	658	22.15
0.2083	10.80	584	21.95
0.1826	10.62	512	21.59
0.1567	10.40	440	21.14
0.1300	10.11	365	20.55
0.1042	9.72	293	19.76
0.0784	9.25	220	18.80
0.0516	8.68	145	17.64
0.0258	7.82	72.4	15.89
0.0133	7.06	37.3	14.35

TABLE 22

PLOTTING DATA FOR UNIVERSAL VELOCITY DISTRIBUTION 7

Re = 30,800
f = 0.0239

u* = 0.583 ft./sec.
U = 10.65 ft./sec.

y (ft.)	u (ft./sec.)	y^+	u^+
0.0133	8.81	44.2	15.11
0.0267	9.48	88.8	16.26
0.0525	10.35	174	17.75
0.0784	10.98	260	18.83
0.1050	11.45	349	19.64
0.1309	11.93	435	20.46
0.1567	12.29	521	21.08
0.1833	12.51	610	21.45
0.2092	12.72	695	21.81
0.2350	12.95	781	22.21
0.2342	12.93	779	22.17
0.2083	12.79	693	21.93
0.1826	12.56	607	21.54
0.1567	12.31	521	21.11
0.1300	11.89	432	20.39
0.1042	11.49	347	19.71
0.0784	10.95	260	18.78
0.0516	10.32	172	17.70
0.0258	9.46	85.8	16.22
0.0133	8.72	44.2	14.95

TABLE 23

RATIO OF BULK VELOCITY TO MAXIMUM VELOCITY FOR FULLY-DEVELOPED PROFILES

Profile No.	Re	U (ft./sec.)	$u_{max.}$ (ft./sec.)	$U/u_{max.}$
1	11,430	3.84	4.82	0.796
2	17,190	5.75	7.04	0.818
3	18,250	6.13	7.54	0.813
4	21,000	7.09	8.68	0.816
5	24,000	8.06	9.84	0.820
6	26,200	8.83	10.85	0.814
7	30,800	10.65	13.04	0.817

TABLE 24

RESULTS OF GRAPHICAL INTEGRATIONS

Traverse No.	$\int_0^{r_w} urdr$ (ft./sec. in.^{2})	ρ (lb./ft.^{3})	U (ft./sec.)	Re	
		Pitot Tube Profiles			
1	18.73	0.0698	3.84	11,430	
2	28.1	0.0699	5.75	17,190	
3	29.9	0.0697	6.13	18,250	
4	34.4	0.0695	7.09	21,000	
5	39.3	0.0696	8.06	24,000	
6	43.0	0.0696	8.83	26,200	
7	51.9	0.0677	10.65	30,800	
		Hot Wire Profiles			
1		0.0690	0.313	925	Re determined from orifice measurement
2		0.0680	0.454	1,320	
3		0.0679	0.580	1,690	
4		0.0690	0.748	2,210	
5		0.0687	0.967	2,840	
6	9.11	0.0690	1.868	5,500	
7	16.00	0.0690	3.28	9,660	

TABLE 25

POINT VELOCITY MEASUREMENTS AT 24.0, 41.2, & 50.8 PIPE DIAMETERS DOWNSTREAM FROM ENTRANCE

- Hot Wire Positioned in Center of Main Flow Pipe 50.8 Dia. Downstream from Entrance -

Pitot Tube Position (Dia. from entrance)	W.R.R.C. Setting (ft.^{3}/min.)	Blower Speed (rpm)	Bar. Press. (psia)	Flowing Temp. (R)	Pitot Tube Press. Diff. (in. alc.)	Hot Wire Current Rdg. (ma.)	u by Pitot Tube (ft./sec.)	u by Hot Wire (ft./sec.)
24.0	40	930	13.40	540	0.0051	92.20	4.53	4.32
24.0	50	930	13.40	536	0.0077	94.05	5.55	5.52
24.0	60	930	13.40	538	0.0110	95.18	6.64	6.60
24.0	75	930	13.40	540	0.0163	96.90	8.10	8.35
41.2	57	910	13.56	539	0.0094	94.80	6.12	6.40
41.2	62	910	13.56	539	0.0112	95.42	6.68	6.96
41.2	68	910	13.56	539	0.0133	95.80	7.28	7.30
41.2	75	1350	13.56	541	0.0181	96.95	8.50	8.35
41.2	85	1350	13.56	542	0.0224	97.75	9.46	9.48

TABLE 26

FRICTION FACTOR DATA

Length for pressure drop measurements = 18.416 ft.

EXPERIMENTAL DATA

Test No.	W.R.R.C. (ft.^{3}/min.)	Blower Speed (rpm)	Flowing Temp. (C)	Bar. Press. (cm. Hg.)	Press.Drop (in. alc.)
1	43	930	20.0	69.82	0.0039
2	61	1050	20.5	68.94	0.0083
3	67	1050	21.0	68.94	0.0097
4	78	1050	21.5	68.94	0.0122
5	87	1325	23.0	68.94	0.0150
6	103	1350	22.0	69.82	0.0180
7	116	1570	24.0	69.82	0.0257

$$f = \frac{2g_c D}{\rho U^2}\left(\frac{-dP_f}{dx}\right) \qquad \frac{-dP_f}{dx} = \frac{-\Delta P}{\Delta L}$$

$$f = \frac{2 \times 32.2 \times 6.255}{\rho U^2 \times 12}\left(\frac{-\Delta P}{\Delta L}\right)$$

$$f = \frac{33.6}{\rho U^2}\left(\frac{-\Delta P}{\Delta L}\right)$$

CALCULATED DATA

Test No.	Re	ρ (lb./ft.^{3})	U^2 (ft./sec.)^2	$-\Delta P/\Delta L$ (lb./ft.^{3})	f
1	11,430	0.0691	15.03	0.000889	0.0287
2	17,190	0.0681	34.6	0.001891	0.0270
3	18,250	0.0680	39.6	0.00221	0.0276
4	21,000	0.0680	52.5	0.00278	0.0262
5	24,000	0.0675	69.0	0.00342	0.0247
6	26,200	0.0687	80.0	0.00410	0.0251
7	30,800	0.0685	110.8	0.00585	0.0259

TABLE 27

HOT WIRE CALIBRATION

Blower Speed - 1350 rpm Bar. Press. - 70.25 cm. Hg. Still Air Rdg. - 327.0

		PITOT TUBE DATA					HOT WIRE DATA			
Test No.	W.R.R.C. Rdg. (ft.^{3}/min.)	Temp. (R)	ρ (lb./ft.^{3})	Δh (in. alc.)	u (ft./sec.)	$\sqrt{\frac{P}{P_o}}\sqrt{u}$	I (ma.)	I^2	Temp. Corr.	Corr. I^2
1	100	545	0.0675	0.0318	11.22	3.36	99.05	9810	-56	9754
2	90	543	0.0678	0.0246	9.84	3.14	97.95	9592	-33	9559
3	80	541	0.0680	0.0195	8.76	2.97	97.27	9462	-11	9451
4	76	541	0.0680	0.0177	8.35	2.89	96.97	9403	-11	9392
5	68	539.5	0.0682	0.0146	7.58	2.76	96.02	9220	5	9225
6	64	539.5	0.0682	0.0131	7.17	2.68	95.62	9143	5	9148
7	59	539.5	0.0682	0.0111	6.60	2.57	95.05	9033	5	9038
8	55	539	0.0683	0.0098	6.20	2.49	94.40	8912	11	8923
9	51	539	0.0683	0.0082	5.66	2.38	94.00	8835	11	8846

TABLE 28

HOT WIRE CALIBRATION

Blower Speed - 1550 rpm   Bar. Press. - 70.31 cm. Hg.   Still Air Rdg. - 327.0

	PITOT TUBE DATA						HOT WIRE DATA			
Test No.	W.R.R.C. Rdg. ($ft.^3$/min.)	Temp. (R)	ρ ($lb./ft.^3$)	Δh (in. alc.)	u (ft./sec.)	$\sqrt{\frac{P}{P_o}}\sqrt{u}$	I (ma.)	I^2	Temp. Corr.	Corr. I^2
1	115	548	0.0672	0.0414	12.90	3.60	100.05	10010	-89	9921
2	110	547	0.0673	0.0377	12.29	3.51	99.62	9925	-78	9847
3	105	546	0.0674	0.0347	11.76	3.44	99.27	9855	-67	9788
4	100	545	0.0675	0.0315	11.18	3.35	99.07	9815	-56	9759
5	95	544	0.0676	0.0283	10.57	3.26	98.57	9715	-44	9671
6	90	543	0.0677	0.0259	10.09	3.18	98.17	9638	-33	9605
7	86.5	542	0.0679	0.0234	9.59	3.10	97.70	9545	-22	9523
8	78	541	0.0680	0.0197	8.80	2.97	97.17	9441	-11	9430
9	74	540	0.0681	0.0175	8.28	2.88	96.77	9363	0	9363
10	68	539.5	0.0682	0.0144	7.52	2.75	96.15	9245	5	9250
11	63	539.5	0.0682	0.0125	7.01	2.65	95.75	9167	5	9172
12	55	539	0.0683	0.0097	6.17	2.49	94.55	8940	11	8951

TABLE 29

CALIBRATION OF 0.375" ORIFICE

Bar. Press. - 70.4 cm. Hg.

Test No.	W.R.R.C. Rdg. ft.^{3}/min.	Temp. (R)	Meter Press. psia	ρ lb./ft.^{3}	Δh cm. H2O	$\frac{\Delta h}{\rho}$	$\left(\frac{\Delta h}{\rho}\right)^{\frac{1}{2}}$	D.M. Vol. ft.^{3}	Corr. Vol. ft.^{3}	Time (sec.)	Flow Rate ft.^{3}/sec.	113.6 Q	C_o
1	17.5	539	13.62	0.0685	6.5	94.9	9.75	5	4.975	70.5	0.0706	8.01	0.823
2	30	539	13.63	0.0685	11.1	162.0	12.73	5	4.975	53.6	0.0928	10.54	0.828
3	40	539	13.64	0.0685	14.8	216.0	14.70	5	4.975	46.5	0.1070	12.14	0.826
4	50	539	13.64	0.0685	18.6	271.5	16.48	5	4.975	41.7	0.1194	13.55	0.822
5	60	539	13.65	0.0686	22.0	320.5	17.90	5	4.975	37.75	0.1320	14.99	0.837
6	70	543	13.67	0.0681	28.1	412.0	20.28	10	9.95	66.95	0.1485	16.88	0.831
7	92	547	13.68	0.0677	33.7	498.0	22.30	10	9.95	61.3	0.1623	18.44	0.826
8	114	549	13.69	0.0676	41.1	608.0	24.63	10	9.95	55.1	0.1807	20.50	0.831
9	149	551	13.70	0.0675	52.4	776.0	27.80	10	9.95	48.9	0.2035	23.10	0.831

Average C_o = 0.828

Orifice Equation Used:

$$Q = C_o A_o \sqrt{\frac{2g_c \Delta P}{\rho}}$$

TABLE 30

EFFECT OF VANES AT Re = 1320

Orif. Press. Drop - 12.0 cm. H_2O
W.R.R.C. - 32.5 ft.^{3}/min. (1.c.)
Orifice - 0.375"
Blower Speed - 910 rpm

Bar. Press. - 69.82 cm. Hg.
Flow Temp. - 25.0 C.
Hot Wire Still Air Rdg. - 327.0
Pt. of Measurement - 50.8 D.

Probe Position (in.)	No Vanes Current (ma. x 4)	With Vanes Current (ma. x 4)
3.06	328.0	327.5
2.96	329.4	328.0
2.86	331.0	330.0
2.76	332.1	330.7
2.66	333.2	332.0
2.50	333.1	333.2
2.19	334.3	334.7
1.88	335.0	334.0
1.56	336.0	334.8
1.25	336.1	335.0
0.94	336.0	334.5
0.63	336.0	334.9
0.31	336.1	335.0
0	336.5	334.8
0.31	336.4	335.0
0.63	336.1	335.0
0.94	335.8	334.8
1.25	335.2	335.1
1.56	334.8	335.0
1.88	334.3	334.8
2.19	333.0	335.1
2.50	331.5	333.0
2.66	330.1	332.2
2.76	329.8	330.7
2.86	329.0	329.0
Still Air	327.0	327.0

TABLE 31

EFFECT OF VANES AT Re = 1690

Orif. Press. Drop - 19.6 cm. H_2O
W.R.R.C. - 52.0 ft.^{3}/min. (1.c.)
Orifice - 0.375"
Blower Speed - 910 rpm

Bar. Press. - 69.96 cm. Hg.
Flow Temp. - 26.0 C.
Hot Wire Still Air Rdg. - 327.0
Pt. of Measurement - 50.8 D.

Probe Position (in.)	No Vanes Current (ma. x 4)	With Vanes Current (ma. x 4)
3.06	328.0	328.0
2.96	329.0	329.0
2.86	331.1	331.6
2.76	333.0	332.6
2.66	335.0	334.5
2.50	336.1	335.7
2.19	337.2	337.1
1.88	337.8	337.6
1.56	338.0	338.0
1.25	338.0	338.0
0.94	338.0	338.0
0.63	338.0	338.0
0.31	337.8	338.1
0	338.1	338.2
0.31	338.1	338.2
0.63	338.0	338.3
0.94	337.8	338.0
1.25	338.0	338.2
1.56	338.1	338.0
1.88	337.9	338.0
2.19	336.9	337.0
2.50	335.7	336.0
2.66	334.8	334.2
2.76	333.0	332.5
2.86	331.0	331.0
Still Air	327.0	327.0

APPENDIX C

Conversion of Equipment for Gas-Solids Flow Measurement

Provision has been made to convert the equipment for studies of the flow of gas-solids mixtures.

A screw auger will introduce solids into the one-inch throat of the inlet venturi nozzle. The screw auger will be powered by a Graham variable speed drive.

The inlet venturi nozzle shown in Plate 1 was machined in seven sections from a mild steel and the sections were joined by electric arc-welding. The nozzle has a side-arm attached which inclines slightly upwards into the one-inch nozzle throat to provide for the entry of solids from the screw feeder. The centerlines of the side-arm and the nozzle throat intersect at an angle of 85 degrees to give a steady solids feed rate. The screw auger will be set back from the nozzle throat so that the solids will be pushed up the incline beyond the auger.

Glass beads (serial number 380-5005) were purchased from the Minnesota Mining and Manufacturing Company, St. Paul, Minnesota for use as the solid phase. The bead properties are listed below.

Shape - spherical

Size - approximately 95% 18-40 microns diameter

Density - 156 lb./ft.^{3}

Bulk Density - 97 lb./ft.^{3}

Calculations based on Stokes law show that for a Reynolds number of 1000 in the main flow pipe, the average gas velocity is equal to the settling velocity of a glass bead of 36 microns diameter in air at 15 psia and 77 F. It is evident that further classification must be made to separate the beads into a cut below 36 microns diameter in order to study air-solids flow at a Reynolds number of 1000 or lower in the main flow pipe.

The solids feed rate versus screw auger rpm may be calibrated with the screw auger in place by allowing the solids to drop through the venturi nozzle. The plug may be removed from the tee just below the nozzle to collect the solids for weighing. The air flow rate is metered by a Foxboro Model M40 Air Weight Controller.

The solids recovery section, shown in Plate 3, of the unit has been completed. It consists of a cyclone separator and a bag filter positioned before the pressure controller valve. The cyclone separator was designed according to Lapple* to remove all of the solid particles from the air-solids mixture under the least favorable conditions, i.e. minimum air velocity corresponding to a Reynolds number of 1000 in the main flow pipe and minimum particle size of 18 microns diameter.

The bag filter was included in the equipment as a precautionary measure to remove any particles not removed by the

---

* "Fluid and Particle Mechanics", C.E. Lapple, First Edition, University of Delaware, Newark, Delaware, 1956.

cyclone separator and thus prevent any loss of solids and also prevent solids from becoming lodged in the pressure controller valve. The experimentally determined pressure drop across the clean bag filter at an air flow rate of 116 cfm was 12 millimeters of mercury.

A 30 foot vertical section of 1 inch galvanized iron pipe between the outlet of the cyclone separator and the solids storage hopper serves as a solids return line. The solids can therefore be recirculated minimizing the need for a shutdown due to a shortage of solids. Provision has been made in the solids return line to sample the solids separated out by the cyclone separator. The valve arrangement will permit a solids sample to be taken without disturbing the operation of the cyclone separator. By sampling the solids being returned to the storage hopper a more clear picture of what is happening in the main flow pipe may be obtained (eg. solids classification and hold-up in main flow pipe).

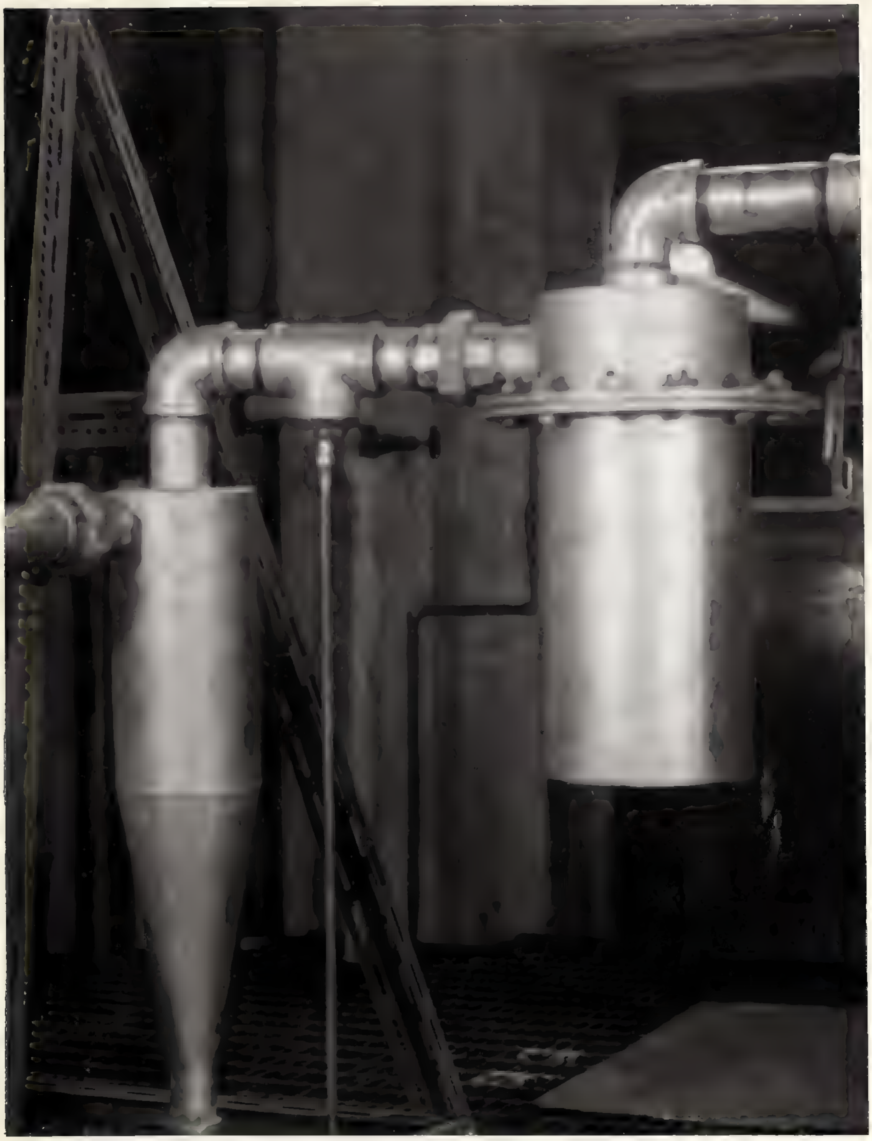

PLATE 3

SOLIDS SEPARATION SECTION

APPENDIX D

The Problem of Sampling an Air-Solids Stream

Various instruments are available for collecting solids from a gas stream and good outlines of these devices are given by Stairmand (1) and by Moore et al (2). The method proposed for use with this system is to sample isokinetically the air-solids stream through a probe and filter arrangement as shown schematically in Figure 16.

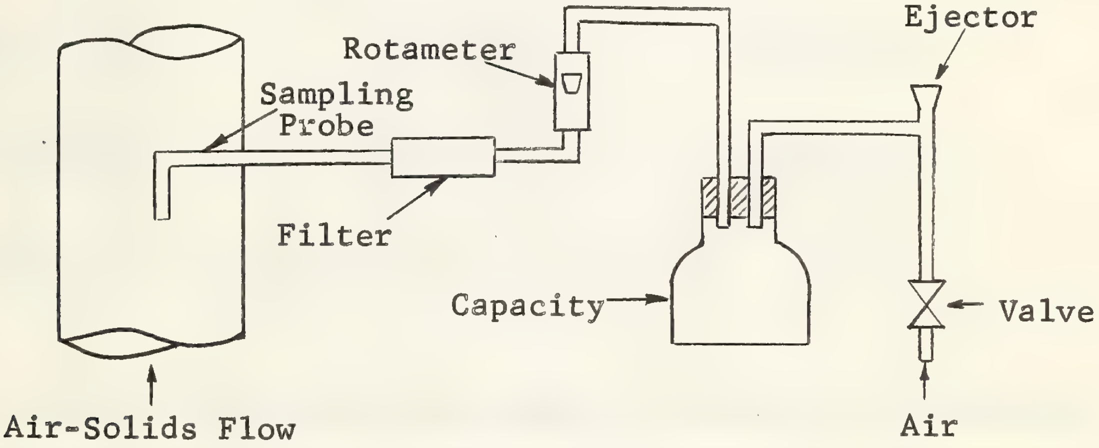

FIGURE 16: Solids Sampling Arrangement

Isokinetic sampling refers to sampling such that the velocity in the probe tip is equal to that in the fluid stream. Watson (3), using powders of 32 and 4 microns diameter in a 10 mph stream, found that isokinetic sampling was necessary to obtain a representative solids sample. Qualitatively it can be seen that sampling with probe inlet velocities greater than the stream velocity result in low measured solids concentrations

and sampling with probe inlet velocities lower than the stream velocity give high solids concentrations because of the solids' inertia. Thus it is necessary to measure and control the rate of air sampling through the probe.

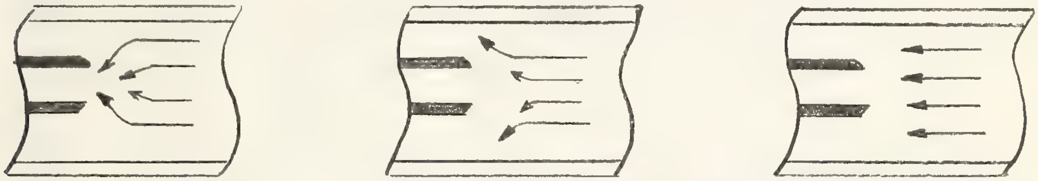

Probe Velocity greater than Stream Velocity-

defficienty of particles

Probe Velocity less than Stream Velocity-

excess of particles

Isokinetic Sampling-

representative sampling

FIGURE 17: Errors due to non-isokinetic sampling

It is evident that the number of bends in the sampling probe should be kept at a minimum to prevent particle loss due to impaction, and horizontal sections of the probe should be avoided if possible since particles may settle out. Doyle (4) summarizes these and other major sources of error and gives recommendations for minimizing the effects of these errors.

Giffith and Jones (3), and Mayhood and Langstroth (3) found that there is a critical probe diameter below which, even under isokinetic conditions, the solids concentration measured will be too low. Their results as shown in Figure 18 show that

for probes having an inside diameter less than about 0.7 cm. (0.275 inches) the solids concentration measured was consistently low.

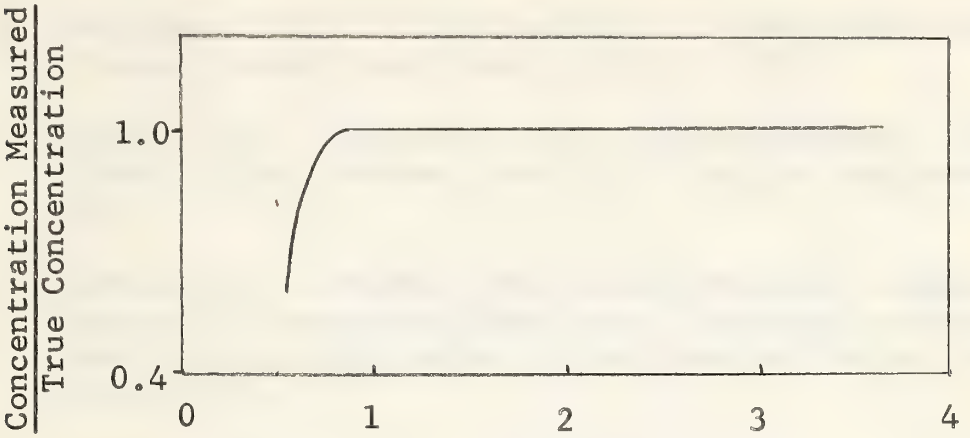

FIGURE 18: Effect of Probe Diameter on Solids Concentration Under Isokinetic Conditions

It is possible, however, that these workers were using blunt nosed probes in which the relatively large values of wall thickness compared to probe inside diameter caused disturbances in the stream which would account for the low values obtained. This appears to be the case since there are examples in the literature (5, 6, 7) of workers using tapered probes which were smaller than this critical limit. For example, Lewis et al (5) used a tapered probe with an inside diameter of 0.09375 inches to measure solids concentration profiles across a duct and found material balances which were in good agreement. It seems to be insignificant whether the probe tip is tapered on the inside or the outside.

BIBLIOGRAPHY FOR APPENDIX D

1. Stairmand, C.J., "The Sampling of Dust-Laden Gases", Trans. Instn. Chem. Eng., 29 : 15, 1951.

2. Moore, C.B., Ehrenfeld, J.R., and Wiederhorn, N.M., "Dust in Gas Streams, Part 2", Pipeline Engineer, July, 1961.

3. Watson, H.H., "Errors Due to Anisokinetic Sampling of Aerosols", Report of Symposium V, Aerosols Chemical and Radiological Laboratory, Army Chemical Center, Maryland, June, 1953.

4. Doyle, A.W., Wiederhorn, N.M. and Swan, A., "Dust in Gas Streams, Part 3", Pipeline Engineer, August, 1961.

5. Lewis, C.H., Petersen, E.E., Acrivos, A. and Tao, G., "A Study of Solid Particle Distribution in a Gas-Solid Jet", Paper Delivered at National Meeting A.I.Ch.E., March 15, 1959.

6. Trotter, I.P., "Point Studies of Mean Flow Properties in Vertical Gas-Solids Transport Systems", Symposium of Dynamics of Multiphase Systems, University of Delaware, December 28-29, 1961.

7. Soo, S.L., and Regalbuto, J.A., "Concentration Distribution in Two-Phase Pipe Flow", Canadian Journal of Chemical Engineering, October, 1960.

B29807